

# Sensor Placement Optimization Study for the Built Environment: Operational Use Cases

March 2025

Stacy Irwin  
Jonathan Napier  
Jacob Inman  
Benjamin McDonald  
Lisa Newburn  
Warnick Kernan  
Chelsea Sleiman



Prepared for the U.S. Department of Homeland Security Science and Technology Directorate under the U.S. Department of Energy Contract DE-AC05-76RL01830, via funding provided on Interagency Agreement 70RSAT23KPM000034.

## DISCLAIMER

This report was prepared as an account of work sponsored by an agency of the United States Government. Neither the United States Government nor any agency thereof, nor Battelle Memorial Institute, nor any of their employees, makes **any warranty, express or implied, or assumes any legal liability or responsibility for the accuracy, completeness, or usefulness of any information, apparatus, product, or process disclosed, or represents that its use would not infringe privately owned rights.** Reference herein to any specific commercial product, process, or service by trade name, trademark, manufacturer, or otherwise does not necessarily constitute or imply its endorsement, recommendation, or favoring by the United States Government or any agency thereof, or Battelle Memorial Institute. The views and opinions of authors expressed herein do not necessarily state or reflect those of the United States Government or any agency thereof.

PACIFIC NORTHWEST NATIONAL LABORATORY  
*operated by*  
BATTELLE  
*for the*  
UNITED STATES DEPARTMENT OF ENERGY  
*under Contract DE-AC05-76RL01830*

Printed in the United States of America

Available to DOE and DOE contractors from  
the Office of Scientific and Technical Information,  
P.O. Box 62, Oak Ridge, TN 37831-0062

[www.osti.gov](http://www.osti.gov)

ph: (865) 576-8401

fox: (865) 576-5728

email: [reports@osti.gov](mailto:reports@osti.gov)

Available to the public from the National Technical Information Service  
5301 Shawnee Rd., Alexandria, VA 22312

ph: (800) 553-NTIS (6847)

or (703) 605-6000

email: [info@ntis.gov](mailto:info@ntis.gov)

Online ordering: <http://www.ntis.gov>

# **Sensor Placement Optimization Study for the Built Environment: Operational Use Cases**

March 2025

Stacy Irwin  
Jonathan Napier  
Jacob Inman  
Benjamin McDonald  
Lisa Newburn  
Warnick Kernan  
Chelsea Sleiman

The research in this presentation was conducted with the U.S. Department of Homeland Security (DHS) Science and Technology Directorate (S&T) under contract 70RSAT23KPM000034. Any opinions contained herein are those of the author and do not necessarily reflect those of DHS S&T.

Pacific Northwest National Laboratory  
Richland, Washington 99354

## Summary

Systems of fixed-position radiation sensors can provide information that assists emergency responders following nuclear and radiological incidents. State, local, tribal, and territorial (SLTT) government agencies that implement systems of fixed-position sensors are faced with numerous decisions regarding sensor selection, quantity, and placement. To develop guidance on implementation of radiation detection systems, we simulated the release of radioactive material in an urban environment using a combination of three models: the Weather Research Forecasting (WRF), Quick Urban and Industrial Complex (QUIC), and Monte Carlo N-Particle (MCNP) models. We then evaluated the performance of several hypothetical sensor systems. The small number of simulations we conducted are not sufficient to generate definitive design guidance for radiation sensor systems, but we did identify trends that would be of interest to emergency planners. For a scenario that releases 1000 curies of Cs-137, radiation detectors were needed at 500-meter intervals to have a high likelihood of event detection and to estimate source location and plume detection. We also noted that optimal detector altitude varied with distance to the source.

We recommend additional research in this area be conducted to support developing sensor placement guidelines that expand on a range of locations, isotopes, activity levels, and different weather conditions. Original simulation strategies included a range of environments, additional radioisotopes (Am241 and AmBe), and a larger selection of sensor types. These types of expansions would support SLTT guidance on sensor system recommendations.

## Acknowledgements

The authors would like to thank the Department of Homeland Security National Urban Science and Technology Laboratory for sponsoring this work and invaluable feedback and guidance.

## Acronyms and Abbreviations

CAD	Computer-aided design
CPAM	Continuous particulate air monitors
CM	Consequence Management
DHS	U.S. Department of Homeland Security
ESRI	Environmental Systems Research Institution, Inc.
FDNY	New York Fire Department
IA	Interagency Agreement
ICRP	International Commission on Radiological Protection
MCNP	Monte Carlo N-Particle transport code
MDA	minimum detectable activity
NaI	Sodium Iodide
NNSA	National Nuclear Security Administration
PAG	Protective Action Guides
PD	Police Department
PNNL	Pacific Northwest National Laboratory
PVT	polyvinyl toluene
QUIC	Quick Urban and Industrial Complex code
RDD	Radiological Dispersion Device
RED	Radiological Exposure Device
SLTT	state, local, tribal, and territorial
SOW	Statement of Work
UTM	Universal Transverse Mercator
WRF	Weather Resource and Forecasting Model

# Contents

- Summary ..... ii
- Acknowledgements ..... iii
- Acronyms and Abbreviations ..... iv
- 1.0 Introduction ..... 1
- 2.0 Assumptions ..... 2
  - 2.1 Sensor System Use Cases ..... 2
  - 2.2 Type of Incident ..... 2
  - 2.3 Assumptions Based on Existing Responder Guidance ..... 3
    - 2.3.1 Personal Radiation Detectors ..... 3
    - 2.3.2 Community Reception Centers ..... 3
  - 2.4 Expected Radioactivity Concern ..... 3
  - 2.5 Radiation Detection ..... 4
    - 2.5.1 Types of Radiation ..... 4
    - 2.5.2 Types of Radiation Sensors Covered by This Analysis ..... 4
    - 2.5.3 Background Radiation ..... 5
    - 2.5.4 Detection Threshold ..... 5
  - 2.6 Modeling Tools ..... 5
  - 2.7 Built Environments ..... 6
    - 2.7.1 Building Materials ..... 6
- 3.0 Modeling Methodology ..... 7
  - 3.1 Sensor Placement Methods ..... 7
    - 3.1.1 Systematic Placement ..... 7
    - 3.1.2 Random Placement ..... 8
    - 3.1.3 Strategic Placement ..... 8
  - 3.2 Limitations ..... 8
- 4.0 Scenario Overview ..... 9
  - 4.1 Geographic Region ..... 9
  - 4.2 Dose Rate Monitoring Locations ..... 10
  - 4.3 Material Release ..... 12
  - 4.4 Activity Dispersal ..... 12
- 5.0 Simulation Results ..... 15
  - 5.1 Sensor Configurations ..... 15
  - 5.2 Additional Dose Rate Calculation ..... 15
  - 5.3 Evaluation Criteria ..... 15
    - 5.3.1 Event Detection ..... 15
    - 5.3.2 Event Confirmation ..... 15
    - 5.3.3 Time to Detection ..... 16

5.3.4	Release Location.....	16
5.3.5	Plume Detection .....	16
5.3.6	Dose Rate Boundaries .....	16
5.3.7	Dose Rate Boundaries .....	16
5.4	Single Detector .....	16
5.5	One Kilometer spacing.....	20
5.6	One Kilometer Spacing, Alternate Configuration .....	22
5.7	Half Kilometer Spacing.....	25
5.7.1	Dose Rates.....	26
5.8	Analysis Based on Activity Levels .....	33
5.8.1	Number of Sensors.....	33
5.8.2	Planar Layouts .....	33
6.0	Recommendations.....	47
6.1	Detector Spacing .....	47
6.2	Detector Altitude .....	47
6.3	Kriging Analysis .....	48
6.4	General Sensor Guidance.....	50
7.0	Conclusion .....	52
8.0	References.....	54
Appendix A – Modeling Methodology .....		A.1
Appendix B – Minimum Detectable Activity .....		B.4
Appendix C – Glossary .....		C.6
Appendix D – MCNP Dose Rate Monitoring Locations.....		D.1

## Figures

Figure 4.1.	Map of simulated region for dispersal scenarios .....	9
Figure 4.2.	Location of detectors simulated in MCNP .....	10
Figure 4.3.	Simulated detector on north side of Washington Square Park (5-WSN-NE). The release point is visible in the lower right.....	11
Figure 4.4.	Simulated detector in median of East Houston Street (LF-HO-E).....	11
Figure 4.5.	Color scale used for all heat map type graphics. On this color scale blue is the lowest value and red is the highest value .....	12
Figure 4.6.	Four timesteps following a release A) 60 seconds, B) 90 seconds, C) 120 second, D) 150 seconds .....	13
Figure 4.7.	Activity by location at 2490 second (41.5 minutes) timestep at elevations of A) ground level, B) 12.5 meters, and C) 37.5 meters above ground .....	14
Figure 5.1.	Single detector at center of zone.....	17
Figure 5.2.	Simulated dose verses time at location 2-HO-E .....	18
Figure 5.3.	Maximum Dose Rates at All Locations.....	19

Figure 5.4. Four detectors spaced one kilometer apart .....20

Figure 5.5. Dose rate over time of detector 1-10-SE .....21

Figure 5.6. Alternate configuration of four detectors spaced one kilometer apart .....22

Figure 5.7. Dose rate over time of detector BW-8-NW .....23

Figure 5.8. Dose rate over time of detector A-8-E .....23

Figure 5.9. Dose rate over time of detector EX-DL-E .....24

Figure 5.10. Configuration of 22 detectors equally spaced 400 to 500 meters apart .....26

Figure 5.11. Dose rate over time of detector 5-8-NW .....27

Figure 5.12. Dose rate over time of detector SV-BK-HE-N .....27

Figure 5.13. Dose rate over time of detector BW-8-NW .....28

Figure 5.14. Dose rate over time of detector BW-BK-NE .....28

Figure 5.15. Dose rate over time of detector 2-8-NE .....29

Figure 5.16. Dose rate over time of detector 2-HO-E .....29

Figure 5.17. Dose rate over time of detector A-8-E .....30

Figure 5.18. Dose rate over time of detector A-HO-E .....30

Figure 5.19. Dose rate over time of detector EX-DL-E .....31

Figure 5.20. Dose rate over time of detector C-HO-W .....31

Figure 5.21. Time for a detector location to observe an activity above 0.25 mrem/hr at ground level .....32

Figure 5.22. Systematic Sensor Placement, Ground Level, 41.5 Minutes after Release, At ground level (top), 12.5 meters (middle) and 37.5 meters (bottom) .....39

Figure 5.23. Random Sensor Placement, Ground Level, 41.5 Minutes after Release, At ground level (top), 12.5 meters (middle) and 37.5 meters (bottom) .....41

Figure 5.24. Random Sensor Placement, Ground Level, 41.5 Minutes after Release, At ground level (top), 12.5 meters (middle) and 37.5 meters (bottom) .....43

Figure 5.25. Fire stations and Police Precincts, Ground Level, 41.5 Minutes after Release, At ground level (top), 12.5 meters (middle) and 37.5 meters (bottom) .....45

Figure 6.1. Cs-137 plot 12 minutes after release .....48

Figure 6.2. Kriging Analysis Using Four Detectors .....49

Figure 6.3. Kriging Analysis Using 500-Meter Detector Spacing .....49

Figure A.1. Top-down views of the MCNP-computed dose rates from a plume dispersion at 30 s at 0.1 m (left) and 90 m (right) elevation above ground ..... A.2

## Tables

Table 5-1. Evaluation of single-detector configuration ..... 18

Table 5-2. Evaluation of four-detector configuration with 1 km spacing .....21

Table 5-3. Evaluation of alternative four-detector configuration with 1 km spacing .....25

Table 5-4. Does a detector configuration with 500-meter spacing meet the evaluation criteria .....33

Table 5-5. Systematic Sensor Placement.....	40
Table 5-6. Random Sensor Placement .....	42
Table 5-7. Random Placement, Alternate Configuration.....	44
Table 5-8. Sensors Placed at Fire Stations and Police Precincts .....	46
Table B-1. Minimum Detectable Activity calculation methods from NUREG-1507 .....	B.4
Table D-1. Locations of determined dose rates during MCNP Modeling .....	D.1

This page intentionally left blank.

## 1.0 Introduction

Fixed-position radiation monitoring systems can be used by emergency responders to assess emergency situations and guide post-release emergency response. The data from these sensors is useful for radiological plume monitoring and supporting health and safety decision-making. System performance is affected by the type and quantity of sensors used; their location, height, and spacing; and their placement relative to buildings and other structures.

Per an interagency agreement between the Department of Homeland Security (DHS) Science and Technology Directorate National Urban Security Technology Laboratory and the Department of Energy Pacific Northwest National Laboratory (PNNL), PNNL has evaluated the performance of a hypothetical system of sensors during a simulated release of radioactive material in an urban environment. PNNL evaluated the system's ability to detect the release and provide real-time situational awareness for post-incident use cases.

This report is the result of PNNL's analysis. It summarizes PNNL's methodology and analysis results. It also contains actionable recommendations for state, local, tribal, and territorial (SLTT) organizations on configuration of fixed-position radiation monitoring systems for post-release response. The recommendations address detector types and quantity; spacing; and placement in urban environments. PNNL focused on scenarios involving radiological dispersal devices (RDD) that release Cs-137. The analysis was based on actual weather conditions that occurred in Manhattan in 2023. We used three models (WRF, QUIC, and MCNP) to simulate weather conditions, particle dispersion, and exposure rates. Due to encountered technical challenges within modeling framework, the simulation scope was limited to a Cs-137 release in lower Manhattan.

Our *Next Steps* report expands our analysis to address a wider range of situations and environments and provide additional guidance to SLTT organizations on designing sensor systems.

Section 2.0 of this report explains our assumptions and rationale that guided our selection of scenarios and simulation parameters.

Section 3.0 of this report describes our simulation methodology. Specifically, it describes how we used the *Weather Research and Forecasting* (WRF), *QUIC*, and *Monte Carlo N-Particle* (MCNP) models to simulate release and dispersal of radioactive materials. Section 3 also describes the technical challenges we encountered and their solutions.

Section 4.0 provides an overview of the simulated scenario. It describes the geographic area, monitoring locations, and radioactive material.

Section 5.0 summarizes the results of a simulation that we ran in lower Manhattan. We describe the movement of radioactive particles and the resulting dose rates.

Section 6.0 contains recommendations to SLTT organizations that are based on the simulation results.

Sections 7.0 and 8.0 contain our final conclusions and references, respectively.

## 2.0 Assumptions

This section outlines PNNL's assumptions when evaluating the problem and developing a method for optimizing sensor placement. The assumptions narrow the scope of the question to an appropriately tractable problem for this effort. The goal is to develop a method for answering the fundamental question of where to optimally place sensors. Future efforts may explore removing some assumptions to examine a greater number of possible scenarios and conditions.

### 2.1 Sensor System Use Cases

Systems of fixed-position radiation sensors support the following use cases:

1. Plume tracking
2. Health and safety monitoring
3. Dose reconstruction.

### 2.2 Type of Incident

PNNL focused on radiological dispersal device (RDD) scenarios in which the RDD released radioisotopes from a single, stationary point. The results are applicable to other types of scenarios, including transportation accidents and incidents related to radiological work. RDD scenarios exercise all three use cases listed in section 2.1 while remaining relatively simple to model.

PNNL did not address the following scenarios:

**Radiological exposure devices (RED) scenarios.** The fixed monitoring system would be useful in an RED scenario for performing dose reconstruction for people who came into close proximity with the RED. However, REDs do not spread contamination, and thus there is no need to track a radioactive plume following the discovery of the RED. An RED scenario would require health and safety monitoring, but to a lesser degree than an RDD case because there is less potential for the RED to change position in an uncontrolled manner (at least, once it has been secured), whereas contamination from an RDD can be transported to different locations well after the initial release, e.g., through resuspension and washout. Because the RED scenario does not exercise all three use cases of the system, it was not chosen for this effort.

**Scenarios involving nuclear facilities, including nuclear power plants, processing facilities, and naval stations with nuclear-powered vessels.** First, the facilities themselves have significant resources for radiation monitoring and nuclear incident response. In the event of a radioactive release from a nuclear facility, facility personnel would staff a command center, evaluate the type and quantity of material released, and provide information on the release to surrounding communities. Second, the source term from a reactor or facility release is typically more complicated to model since such scenarios involve many fission products, some of which act as parents for additional fission products, meaning that the radiation exposure level is complex and fluctuating. Finally, the placement criteria derived from analyzing RDD scenarios will likely be suitable for evaluating releases from nearby nuclear facilities since both involve

plumes of radiation that will settle onto the ground and require plume tracking, health and safety monitoring, and dose reconstruction.

**A nuclear detonation.** Modeling dispersion of radioactive contamination from nuclear detonations is more complicated than modeling an RDD due to the greater number of distinct radionuclides, the potential for neutron activation, and the possibility that the blast drives radioactive contamination high into the atmosphere. A nuclear detonation scenario is thus much more difficult to model than an RDD scenario.

## 2.3 Assumptions Based on Existing Responder Guidance

For this work, PNNL is assuming that local jurisdictions are following other published DHS first responder guidance regarding radiological incident preparedness. The *Radiological Dispersal Device (RDD) Response Guidance* document (DHS, 2017) provides a basis for response that PNNL assumes will be in place.

### 2.3.1 Personal Radiation Detectors

Many first responders will have personal radiation detectors. This assumption will be incorporated into the placement of radiation sensors and may mean it is less critical to place them in ground-level configurations.

### 2.3.2 Community Reception Centers

Local jurisdictions will establish community reception centers where people will be assessed for exposure and contamination and registered for radiological assessment if needed (DHS, 2017). Consequently, the fixed-position radiation monitoring system does not need to be capable of quantifying radionuclides for internal dose reconstruction, which often includes radionuclides that primarily emit alpha and beta radiation. The system thus only needs to support quantifying contributions from external dose, which is primarily through gamma and x-ray exposure. This means that air sampling equipment used to quantify alpha and beta radiation emissions is not needed for this system.

## 2.4 Expected Radioactivity Concern

Analysis results came from a single RDD scenario. The simulation addresses only one chemical species of the radionuclide to simplify the model. The simulated radionuclide is Cs-137. Cs-137 is commonly used in irradiators and to calibrate radiation detection equipment. There have been several unintended releases of Cs-137 over the past forty years, including the 2019 incident in Seattle (NNSA, 2020).

Cs-137 emits a mid-range energy gamma (662 keV), which is commonly used to calibrate radiation detection equipment. Because Cs-137 has a relatively long half-life of 30.05 years and the timescales for emergency response are measured in days or months, our simulations assume that activity levels are unaffected by radioactive decay.

PNNL modeled activity levels that are sufficient to trigger early-phase protective action guidelines for sheltering in place or evacuation. This protective action guideline is reached at a projected dose of greater than 1 rem (10 mSv) in the first four days, which corresponds to a dose rate of about 10 mrem / hour (EPA, 2017).

## 2.5 Radiation Detection

### 2.5.1 Types of Radiation

Alpha-particle emissions typically travel only a few centimeters in air, with the specific distance depending on alpha-particle energy, air humidity, air density, and other specific factors. Alpha particles barely penetrate (less than 0.1 mm) into materials such as plastics or metals that typically surround radiation detectors. Air samplers that collect and concentrate radioactive particulates on filters are required to effectively detect alpha particles in plumes. Air samplers are not practical for use as unattended sensors because the filters must be changed periodically and may clog over time with ambient particulates (e.g., dust and smoke).

Depending on their energy level, beta particles may travel tens of centimeters or up to several meters in air. They can travel up to one centimeter in water or human tissue. Although they have more penetrating power than alpha particles, air samplers are still required to effectively detect beta particles in plumes. Reliance on beta-particle detection presents the same drawbacks as alpha-particle detection.

Neutrons can travel up to approximately one kilometer in air. Neutrons are generally produced by fission reactions and emitted by few radionuclides. Neutrons would be emitted by an improvised nuclear device at the point of detonation, but we do not expect significant neutrons to be emitted from particles in a radioactive plume (unless the plume contains Am-241 and Be-9, which in combination act as a neutron source).

Gamma rays and X-rays (commonly combined to just gamma rays) are high-energy photons that can travel from meters to kilometers in the air and penetrate up to several meters through solid materials, depending on the photon's energy and the density of the solid material. A variety of detectors are suitable for gamma ray detection. Not all radionuclides emit gamma rays. Nevertheless, due to their penetrating power (which translates into increased range of detection), the wide range of gamma-ray detectors, and the suitability of gamma detectors for unattended use, this study will focus on the evaluation of gamma-ray detectors. Many such detectors are also commonly referred to as dose rate instruments since external dose rate measurement is primarily focused on gamma rays.

### 2.5.2 Types of Radiation Sensors Covered by This Analysis

We use several terms in this report to describe radiation monitoring equipment. The term *detector* describes the part of a radiation sensor that interacts with incoming radioactive particles. The term *instrument* refers to the entire piece of radiation monitoring equipment, including the detector, electronics, display, etc. We use the term *sensor* interchangeably with *instrument*.

PNNL's analysis assumes that fixed position sensors are capable of detecting X-rays and gamma rays, and that they provide count and dose rate information. Instruments with Geiger Mueller or sodium iodide detectors can both provide this information. Instruments should provide continuous data for plume tracking and health and safety monitoring. We excluded continuous particulate air monitors (CPAM) due to their maintenance requirements and potentially longer response times.

To manage the scope of our analysis, we also excluded analysis of instruments that provide information on energy spectra. Energy spectra are useful for identifying the specific

radioisotopes involved in a radiological incident, but more expertise is required to interpret their results.

### 2.5.3 Background Radiation

All instruments have static baseline conditions that they report. This is from background radiation that occurs naturally from terrestrial or cosmic sources. Because of this natural activity, there is always a minimum detectable activity (MDA) that must be crossed to confirm that natural background is supplemented by artificial radiation.

Background will activity fluctuate for a specific location over time based on certain environmental characteristics. These include weather, day night cycle, and presence of radioactive material in construction materials, and nearby use of radioactive material for industrial or medical purposes.

For our simulations, we assume that the natural background radiation is approximately 0.006 mrem per hour. Per the Environmental Protection Agency's RadNet dashboard (EPA, 2025), background radiation levels for New York City typically fluctuate around 0.005 or 0.006 mrem per hour. See 8.0Appendix B for full minimum detectable activity details.

### 2.5.4 Detection Threshold

For a radiological event to be detected, the increase in an instrument's count rate must be greater than increases that could be caused by normal fluctuations in background radiation. For small increases in count rate, more time is needed to verify that the increase is not due to fluctuating background radiation. For this analysis, we assume that a radiological event has been detected if the count rate measured by a detector corresponds to a dose rate of 0.025 mrem per hour. This dose rate corresponds to approximately a four-fold increase over normal background increase over normal background levels. We expect that a four-fold increase would be promptly identified. Note that preventative radiological or nuclear detection interdiction thresholds may be different than the thresholds used in this research. The thresholds in this report are for consequence management (CM) activities.

## 2.6 Modeling Tools

PNNL used three tools to simulate the effects of an RDD.

- Weather Resource and Forecasting Model (WRF): The WRF model was developed by the National Center for Atmospheric Research. The WRF model provides actual weather conditions for specific dates, which are used as inputs for the Quick Urban and Industrial Complex (QUIC) model (Skamarock et. al., 2019).
- Quick Urban and Industrial Complex (QUIC) Dispersion Modeling System: The QUIC model was developed by the Los Alamos National Laboratory and the University of Utah. It simulates the dispersal of radioactive materials and incorporates building geometries (Nelson & Brown, 2013).
- Monte Carlo N-Particles (MCNP): The MCNP model was developed at the Los Alamos National Laboratory. Using building geometry and plume positions generated by the QUIC model, the MCNP model simulated the detection of radioactive particles by various sensor configurations (Kulesza et. al., 2022).

## 2.7 Built Environments

PNNL conducted plume and radiation transport modeling in a dense urban environment. Building positions and heights were retrieved from open-source datasets. The building information was incorporated into QUIC and MCNP models and used for dispersion and radiation transport modeling. The model focused on the dense multi-story buildings of Lower Manhattan.

### 2.7.1 Building Materials

Accurately modeling the materials in every building is not feasible. For the MCNP radiation transport model, PNNL modeled buildings using a single aggregate material approach. The three approaches that were considered are:

- **Perfect attenuators:** Model building objects as ideal gamma-ray attenuators.
- **Material sampling:** A single material is used in all buildings, and simulations are repeated for various building materials. The simulation results are averaged across all materials.
- **Single aggregate material:** A pseudo-material is constructed by averaging all potential building materials. All buildings are modeled with the pseudo-material.

## 3.0 Modeling Methodology

For our simulations, detailed city layouts were imported into QUIC, and meteorological data from WRF was used to simulate wind patterns affecting particle dispersion. The radioactive release was characterized by isotope type, source location, activity level, and other factors. The QUIC model then simulated how the radioactive particles dispersed through the urban environment, taking building geometry into account. We did not simulate building entrances or ventilation systems, so all radioactive particles remained outside the simulated buildings. The positions of all radioactive particles for all simulated time steps were then forwarded to the MCNP model.

Next, the MCNP model calculated the gamma-ray flux and radiation dose rates for different locations and times. The dose rates calculations incorporated all dispersed radioactive particles, including particles that were still airborne and particles that had deposited on buildings and on the ground. The MCNP model also accounted for buildings' shielding effect. The results showed areas with high and low radiation exposure, influenced by buildings acting as shields.

Overall, the combination of MCNP and QUIC provided a comprehensive method for modeling and analyzing radiological dispersion and helped identify effective sensor placement strategies. Reference 8.0 Appendix A for full methodology details.

### 3.1 Sensor Placement Methods

The method of selecting locations for sensor placement is similar between all potential methodologies with a few key differences. The three methods used in this study are discussed in the following sections.

#### 3.1.1 Systematic Placement

Systematic placement is a widely used sampling method that involves selecting locations in an ordered grid at regular intervals. This method is particularly valued for its simplicity, efficiency, and ease of implementation. Systematic placement involves an approach using the following steps:

1. Determination of the area of interest.
2. Determination of the number of sensors to be placed in the area of interest.
3. Identification of the grid spacing method for placement of sensors. This can use square, triangular or rectangular spacing methods.
4. Placement of sensors at those locations to provide uniform coverage throughout the area of interest.

This method allows for a uniform spacing of sensors placed in a simple manner requiring minimal effort but uniform coverage. It provides a cost-effective manner for placement that can be quickly implemented. However, it can introduce sampling bias if the distance between sensors is too great or if sensors are ultimately placed in areas that do not represent the remaining area.

### 3.1.2 Random Placement

Random placement is a methodology that involves choosing locations at random to place sensors within an area of interest, ensuring that each location is equally likely to be selected. Random sampling involves an approach using the following steps:

1. Determination of the area of interest.
2. Determination of the number of sensors to be placed in the area of interest.
3. Random selection of placement locations for sensors.
4. Placement of sensors at the randomly selected locations.

Random selection can be completed using automated tools to ensure any source of placement bias is removed during location selection. This prevents areas from being overlooked due to unexpected or unknown biases formed by a sensor location selector. However, it can introduce areas or corridors throughout an area that may have a limited number of sensors.

### 3.1.3 Strategic Placement

Strategic placement is a method that is frequently used to focus limited scope or purpose driven.

1. Determination of the area of interest.
2. Determination of the number of sensors to be placed in the area of interest.
3. Identification of location of interest.
4. Placement of sensors at the selected locations.

Strategic locations are those that are under control of the sensor operator. Strategic placement is intended to minimize the coordination with stakeholders external to the sensor operators. Strategic placement may be confused with random placement if the methodology for selection isn't known.

## 3.2 Limitations

There are limitations with the modeling and results contained within this document. The project team was only able to provide in-depth analysis of a single dispersal event at a single type of urban environment. This prevents thorough review of impacts of changing wind speed, wind direction, the impact of the physical built environment, type of material released, and method of release were not incorporated into the analysis. This does not prevent general guidance to be generated from its results, however it may allow unique occurrences that would impact recommendations for specific locations to be unobserved.

## 4.0 Scenario Overview

The completed modeling results in two different types of information, dose rate and deposited activity. These were used during analysis during further simulation of sensor response.

### 4.1 Geographic Region

Figure 4.1 shows the region of lower Manhattan that we modeled in our simulations. The grey rectangles are buildings that were modeled in QUIC and MCNP. The release location was the red circle in Washington Square Park. Dark blue circles are locations where we calculated dose rates.

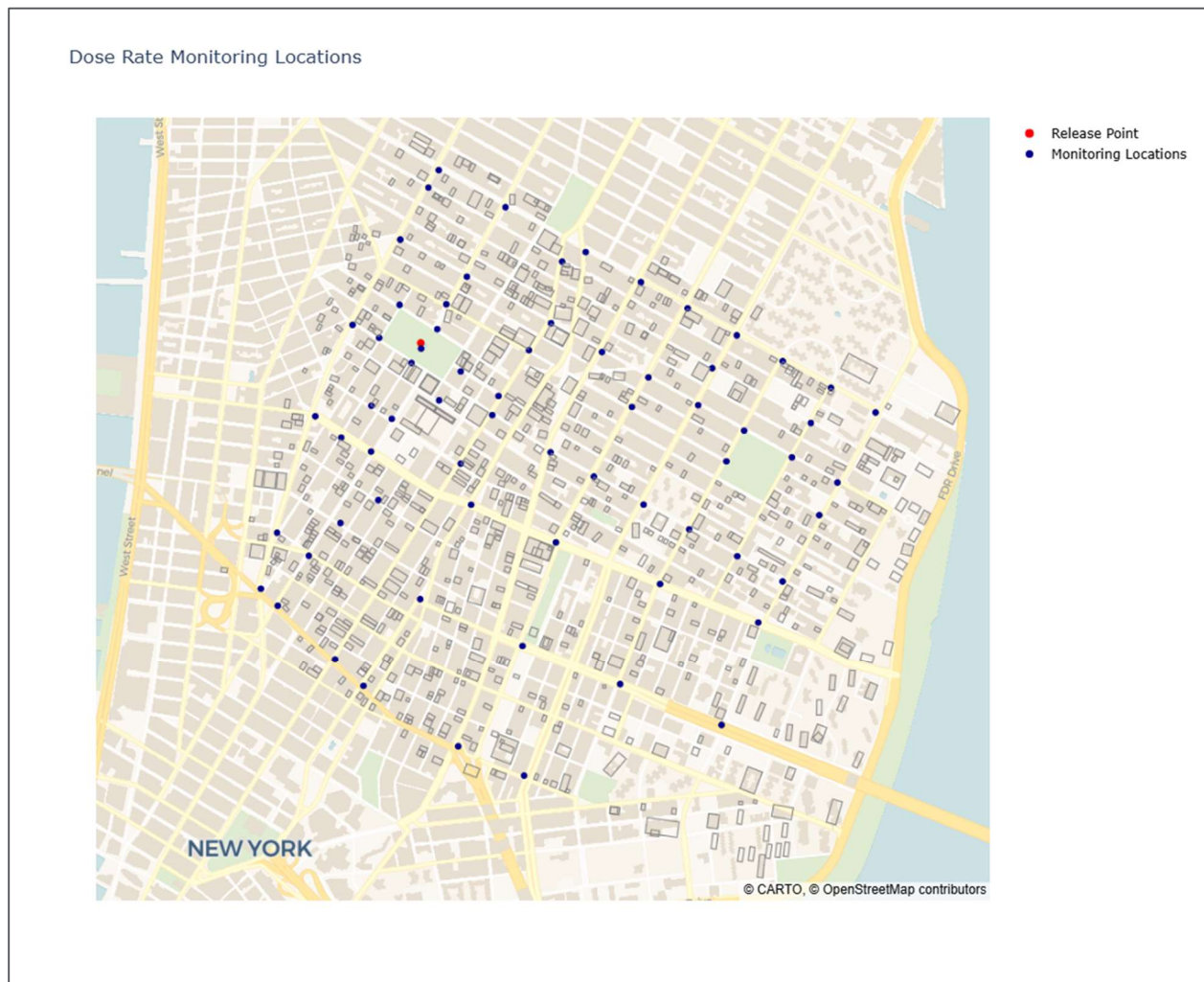


Figure 4.1. Map of simulated region for dispersal scenarios

Figure 4.1 reveals that our simulation framework does not model all the buildings present in this area of lower Manhattan. To manage computational workload, the QUIC model eliminates buildings that it determines will have less impact on plume dispersion. Our results may differ somewhat from how an actual plume would behave in this location. However, we expect that





Figure 4.3. Simulated detector on north side of Washington Square Park (5-WSN-NE). The release point is visible in the lower right

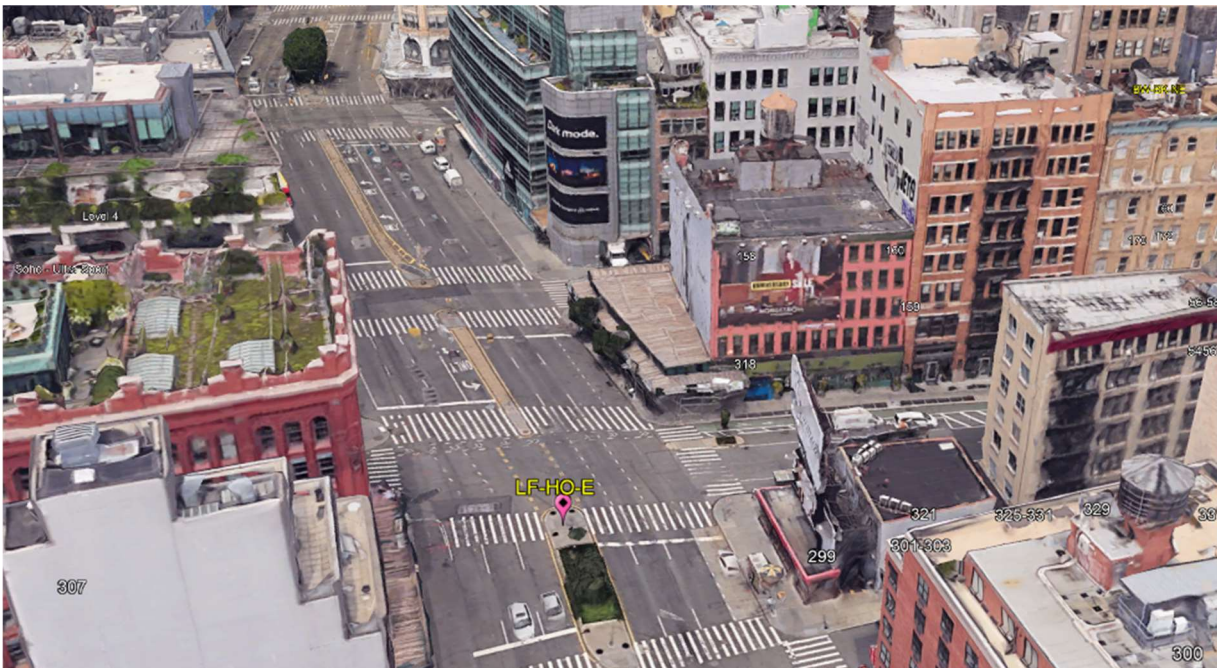


Figure 4.4. Simulated detector in median of East Houston Street (LF-HO-E)

### 4.3 Material Release

The project team reviewed three separate release events to model dispersal of material. Simulations #1 and #2 used real weather data from September 14, 2023. For simulation #3, the wind data was adjusted to contain the plume within the simulation area for a longer time period.

#### Scenario #1

- 14 Sept 2023
- Wind: From the north (23.4°) at 12.4 mph.
- Used High Explosive

#### Scenario #2

- 14 Sep 2023
- Wind: From the north (23.4°) at 12.4 mph.
- No High Explosive

#### Scenario #3

- 14 Sep 2023
- From the northwest (310°) at 2.4 mph.
- No High Explosive

Of the 3 scenarios, scenario #3 provided the best plume characteristics for analysis and was selected for further review. This scenario increased the dispersal of material within the zone of simulation.

### 4.4 Activity Dispersal

**Note:** For this and all subsequent sections, many of the figures use a color scale gradient to demonstrate low to high values. This color scale uses dark blue as the lowest value and deep red as the highest value. All generated figures use this same color scale. Blue is always intended to indicate values at or near background activity or dose rate though the maximum value may change between figures.



Figure 4.5. Color scale used for all heat map type graphics. On this color scale blue is the lowest value and red is the highest value

The modeling tools described in Section 2.5.4 generated spatially representative activity data over the time of the modelling run. The modelling runs simulated a release at ground zero and determined the particle dispersion over the length of the modelling run at 30 second intervals.

Activity was determined in three dimensions at each 30 second interval. An example of this is shown in Figure 4.6 (See Figure 4.5 for an explanation of the color scale). The figure shows four timesteps of 60-, 90-, 120-, and 150-seconds post release and the dispersion of material at each time point. The data points are only scaled to maximum activity for representative purposes in this figure, with red being highest activity. Black dots indicate absence of activity.

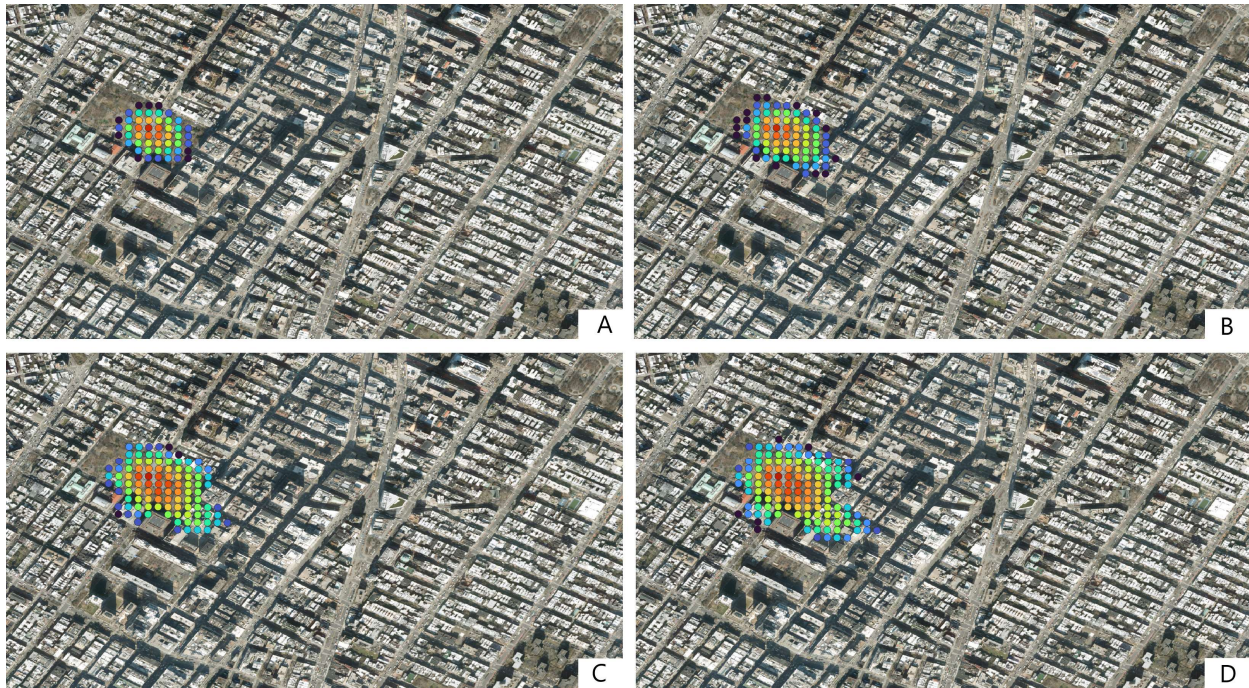


Figure 4.6. Four timesteps following a release A) 60 seconds, B) 90 seconds, C) 120 second, D) 150 seconds

This modelling ran to 9000 seconds (2.5 hours) post release, generating datapoints for every 30 seconds to create a hypothetical plume for analysis. The plume was calculated every 12.5 meters from 0 to 187.5 meters above ground. This vertical component was included in the analysis. An example of the difference in activity is shown in Figure 4.7, which shows the activity at three heights of 0, 12.5, and 37.5 meters. The timestep chosen for this example is 2490 seconds (41.5 minutes). This timestep was chosen to maximize the number of nonzero data points. The datapoints in the figure are scaled to the maximum activity and shown for demonstrative purposes only.



Figure 4.7. Activity by location at 2490 second (41.5 minutes) timestep at elevations of A) ground level, B) 12.5 meters, and C) 37.5 meters above ground

## 5.0 Simulation Results

This section reviews the simulation results and evaluates the performance of seven hypothetical sensor placement strategies. The project team focused on scenario 3, described in Section 4.3. This scenario used no high explosive for dispersal of radioactive material and a wind speed of 2.3 miles per hour.

### 5.1 Sensor Configurations

The sensor placement strategies analyzed are:

1. A single detector.
2. One kilometer spacing
3. Alternate one kilometer spacing
4. 500-meter spacing.
5. Random Placement
6. Systematic Placement
7. Strategic Placement

Strategies 1 through 4 were evaluated using calculated dose rates. Strategies 5 through 7, which were evaluated using Cs-137 particle concentrations, are discussed in Section 5.8.

### 5.2 Additional Dose Rate Calculation

The MCNP model can calculate the density of Cs-137 gamma rays at every location within our simulation area, but additional calculations are needed to convert the gamma ray densities into dose rates. We calculated dose rates verse time at the locations specified in Figure 4.2.

### 5.3 Evaluation Criteria

We chose seven criteria for evaluating the performance of sensor systems.

#### 5.3.1 Event Detection

A sensor system successfully detects an RDD release if at least one instrument sees an increase in dose rate of at least 0.025 mrem per hour, which is approximately a four-fold increase over background radiation levels. The 0.025 mrem per hour threshold is high when compared to the values generated by the MDA calculations discussed in Section 2.5.3, but lower than radiation levels that are related to protective action guidelines (see Section 2.5.4 and EPA, 2017).

#### 5.3.2 Event Confirmation

Detecting elevated dose rates on more than one instrument provides confidence that the elevated dose rates are not due to a system fault (e.g., short circuit) or a normally occurring source of radiation (e.g., a nuclear medicine patient passes by the detector).

### 5.3.3 Time to Detection

Faster detections are preferable.

### 5.3.4 Release Location

Does the sensor system allow first responders to estimate the source of the radioactive release?

### 5.3.5 Plume Detection

Does the sensor system indicate the direction in which the plume is traveling?

### 5.3.6 Dose Rate Boundaries

Early phase protective action guidelines (EPA, 2017) suggest setting up hot zone boundaries at 10 mrem per hour and excluding emergency responders from areas that exceed 10 rem per hour.

### 5.3.7 Dose Rate Boundaries

Early phase protective action guidelines (EPA, 2017) suggest considering shelter-in-place or evacuation actions at doses of 1 to 5 rem over the first four days.

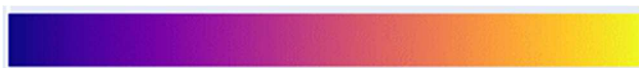
## 5.4 Single Detector

Suppose our simulation area contains a single detector at the center of the zone. The detector is at location 2-HO-E, 970 meters southeast of the release point, in the median of East Houston Street. Figure 5.1 shows the detector location.

Figure 5.2 plots dose rate in mrem per hour versus altitude and time. The maximum dose rate at location 2-HO-E was 0.036 mrem per hour, at an altitude of 137meters. This altitude exceeds the building heights at that location. The maximum dose rate near ground level is 0.13 mrem per hour. We are assuming that an increase of 0.13 mrem per hour is promptly identifiable.

**Note on Color Scales:** The plots in section 5 use two new color scales. The scales' minimum and maximum values vary from plot to plot.

**Dose Rate versus Time Plots:** The color scale ranges from deep purple at the low dose rates to bright yellow at the high dose rates.



**Detector Maps:** Bright yellow is difficult to see against the map backgrounds, so for maps we used a color scale that ranges from blue at low dose rates to red at high dose rates.



The uncolored areas of Figure 5.1 indicate where the dose rate was lower than 0.025 mrem/hr. Natural background radiation in Manhattan is typically between 0.005 and 0.01 mrem/hr, leading to the assumption that dose rates below 0.025 mrem/hr might not be recognized, at least not promptly. Figure 5.1 shows that there is no detectable increase in dose rate until nearly eleven minutes after the release. Dose rates are detectable at higher altitudes before they are detectable near the ground.

Figure 5.1 indicated that activity levels were highest at ground level. In other words, Figure 5.1 suggests there are more radioactive Cs-137 particles near the ground than at higher altitudes. This may appear to be inconsistent with Figure 5.2, which shows higher dose rates at higher altitudes. However, Figure 5.1 showed the distribution of Cs-137 particles at 41.5 minutes after the initial release of material, while Figure 5.2 only extends out to 20 minutes after 20 minutes after release. Most of the Cs-137 that was still airborne had moved out of the simulation area by 40 minutes after the release, leaving only the Cs-137 particles that had deposited onto the ground and buildings.

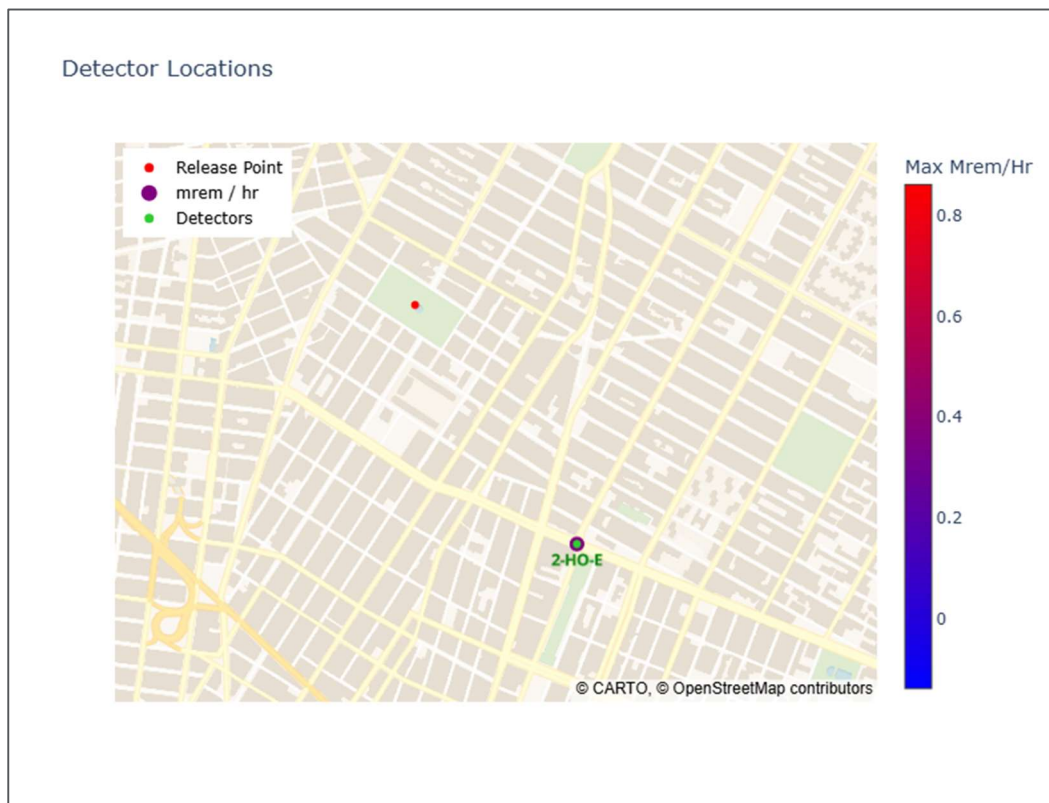


Figure 5.1. Single detector at center of zone

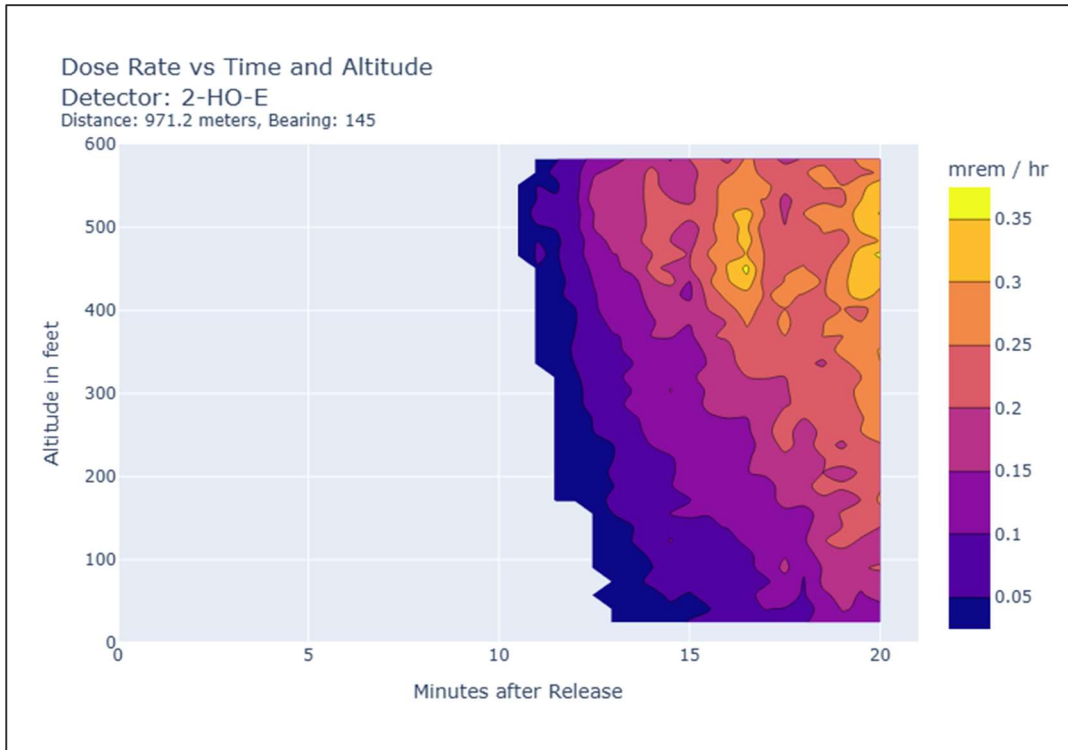


Figure 5.2. Simulated dose verses time at location 2-HO-E

Table 5-1. Evaluation of single-detector configuration

Criteria	Results
Event Detection	Yes 0.025 to 0.15 mrem / hour at ground level
Event Confirmation	No Only one detector
Time to Detection	13 minutes at ground level
Release Location	No data from sensor system Based on wind direction, to the west Distance unknown
Plume Direction	No data from sensor system Based on wind direction, to the east
Dose Rate Boundaries (10 R / hr, 10 mr / hr)	No data from sensor system
Dose Estimates (5R, 1R in first 4 days)	Sensor system is not helpful At least 10 mrem at ground level (assuming 0.1 mrem / hr), but no indication of worst-case dose rate

It's possible to detect that a radioactive release occurred with this single detector. But with only one sensor in our system, we cannot rule out a local anomaly or equipment fault as the cause of the high reading. Furthermore, a single detector provides no indications of the location of the release or the plume direction. Although we could correctly conclude that the plume is traveling west, and the release was to the east of the detector if we knew the wind direction.

A single detector does not help us estimate the size of the release or estimate the dose rates near the release location. The dose rates could have been generated by a small release near the detector, or a large release farther away. With respect to dose rates throughout the affected area, we know that the maximum dose rate is at least 0.1 mrem per hour, which corresponds to 9.6 mrem over four days. This dose rate is well below the early phase PAG for sheltering in place or evacuation (1 to 5 REM over 4 days). Incident responders will need to send personnel with portable radiation detectors into the affected area to identify the range of dose rates.

In this scenario, our instrument successfully identified a radiological event. However, it's important to note that we got lucky.

Figure 5.3 shows all 67 possible detector locations and indicates which detectors would have seen greater than a 0.025 mrem per hour increase. Thirty of the 67 locations did not see any increase in dose rate greater than 0.025 mrem per hour. We intentionally placed release point on the upwind side of the simulation zone so we could observe the plume's movement. This caused the plume to move across a significant portion of our zone, but there is no reason to believe a real event would cooperate with our detector placement.

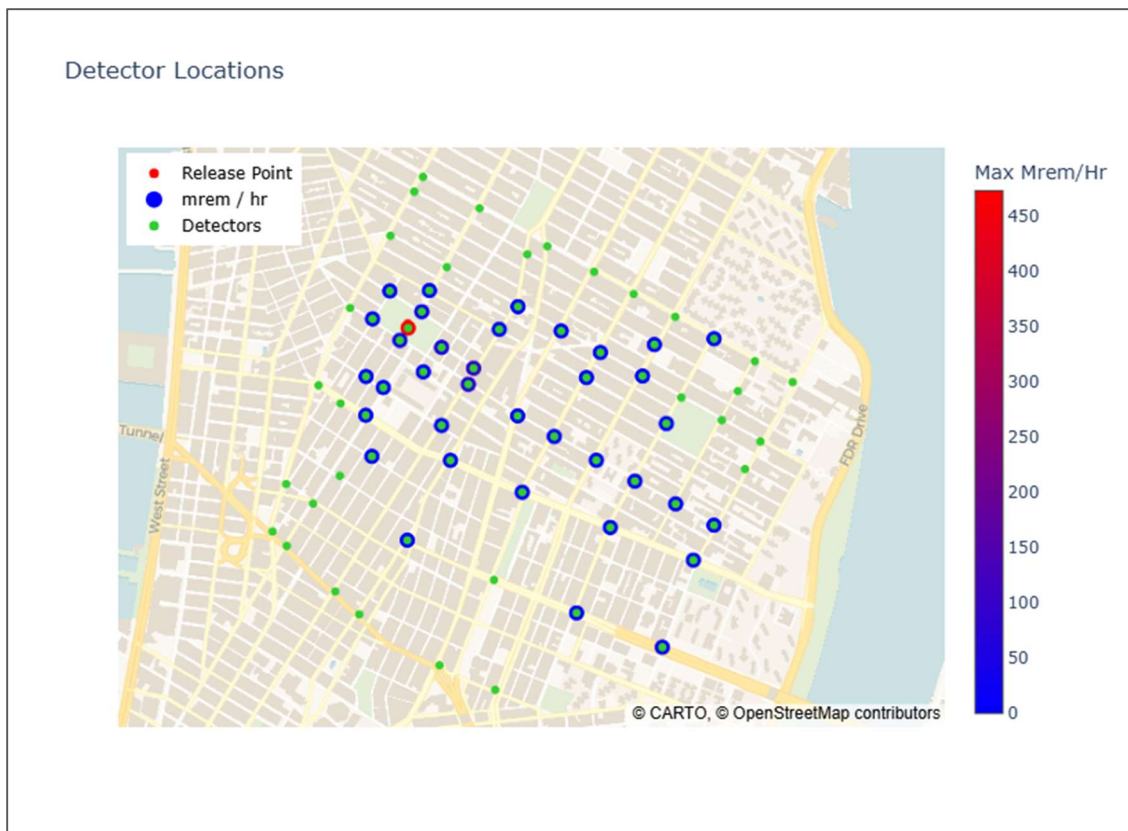


Figure 5.3. Maximum Dose Rates at All Locations

## 5.5 One Kilometer spacing

Increasing the number of detectors may improve results. Figure 5.4 shows four detectors located roughly at the corners of a 1 km by 1 km square, which is a plausible configuration for systems with 1 km spacing between detectors. The detector IDs are 5-10-SE, 1-10-SE, WBS-BK-HE-N, and CH-DL-E.

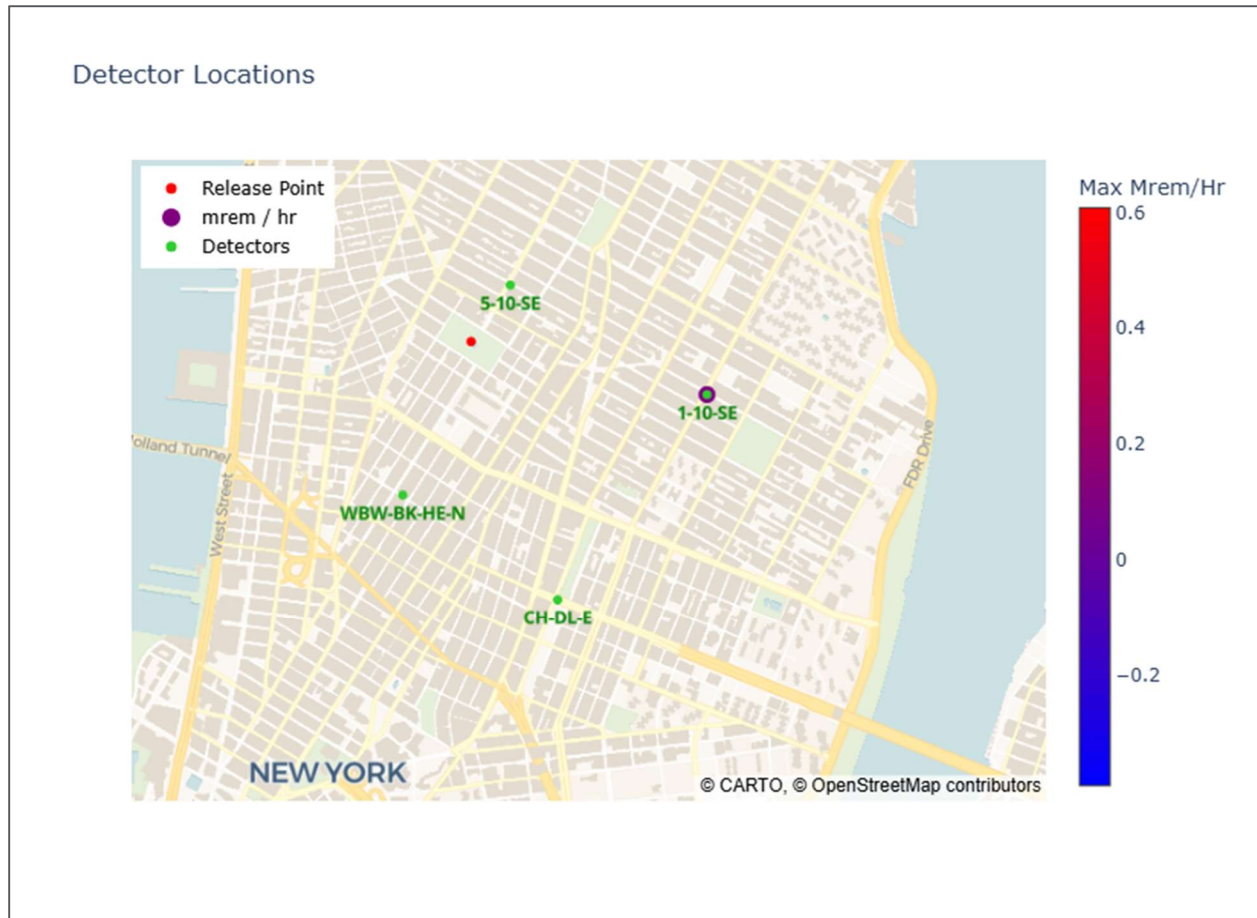


Figure 5.4. Four detectors spaced one kilometer apart

Only detector 1-10-SE in the northeast corner of the square gets a detection.

As shown in Figure 5.5, the first detectable dose rates occur at altitudes greater than 122 meters, 17 minutes after the release. Dose rates are detectable 20 minutes after the release as low as 58 meters. Unless the detector is mounted on a structure that's at least 60 meters tall, an instrument system with 1 kilometer spacing could fail to detect a 1000 Curie release.

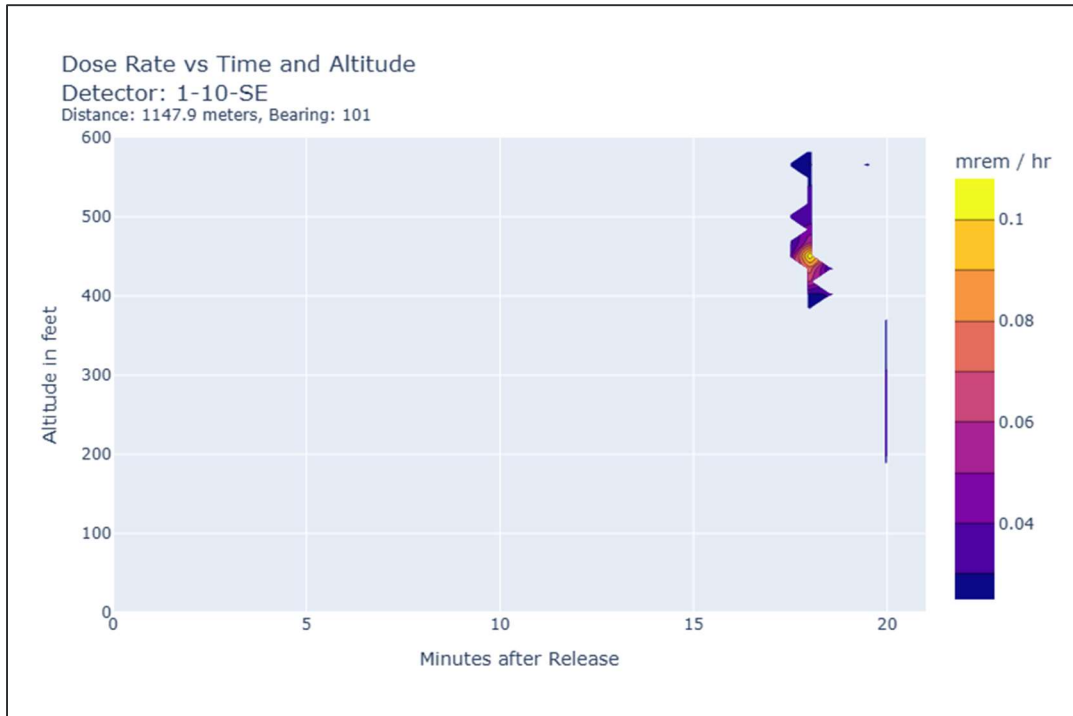


Figure 5.5. Dose rate over time of detector 1-10-SE

The performance of this system with one kilometer spacing is similar to the single detector system.

Table 5-2. Evaluation of four-detector configuration with 1 km spacing

Criteria	Results
Event Detection	No 0.025 to 0.15 mrem / hour at ground level
Event Confirmation	Yes Only one detector
Time to Detection	17 minutes at greater than 122 meters
Release Location	No data from sensor system Based on wind direction, to the west Distance unknown
Plume Direction	No data from sensor system Based on wind direction, to the east
Dose Rate Boundaries (10 R / hr, 10 mr / hr)	No data from sensor system
Dose Estimates (5R, 1R in first 4 days)	Sensor system is not helpful At least 10 mrem at ground level (assuming 0.1 mrem / hr), but no indication of worst-case dose rate

## 5.6 One Kilometer Spacing, Alternate Configuration

There are many combinations of four detectors with one kilometer spacing that can be selected from our set of monitoring locations. In this section, we analyze outputs from a different set of four detectors. The overview plot in Figure 5.6 suggests there could be detection at all four detectors, albeit very slight. However, when we look at the detailed dose rate information for all four detectors, we see that only one location provides a persistent detection near ground level.

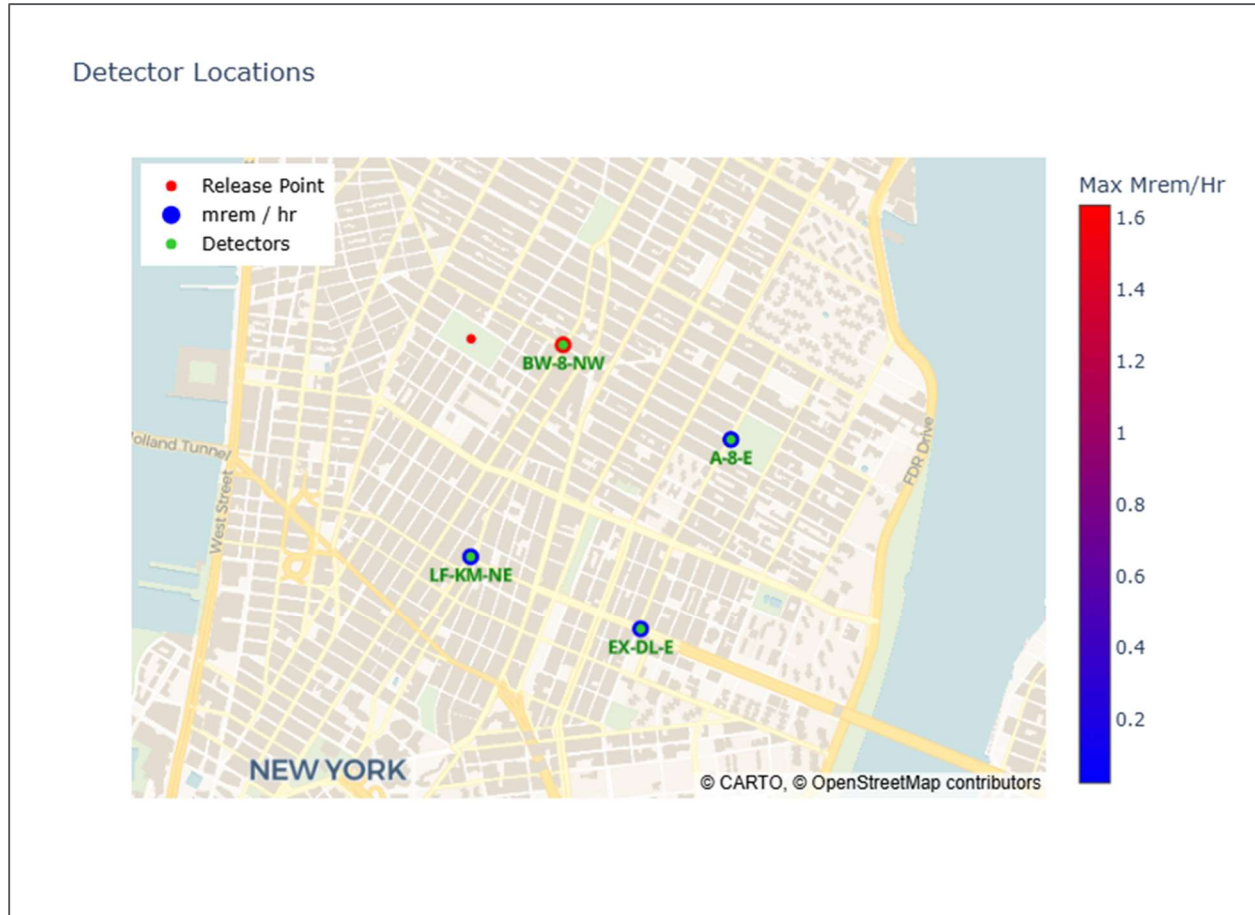


Figure 5.6. Alternate configuration of four detectors spaced one kilometer apart

Figure 5.7 through Figure 5.9 show the dose rates versus time and altitude for three of the four detectors, in ascending order by distance from the release point. The detector at location LF-KM-NE is not shown because there is only one data point greater than 0.025 mrem per hour for that detector (0.027 mrem per hour at an altitude of 87 meters, 20 minutes after the release).

Of the four detectors, only the detector at BW-8-NW has a detection near ground level. For a system of ground-level detectors, only the detector at BW-8-NW would show a detection, making the performance of this system similar to the two prior configurations.

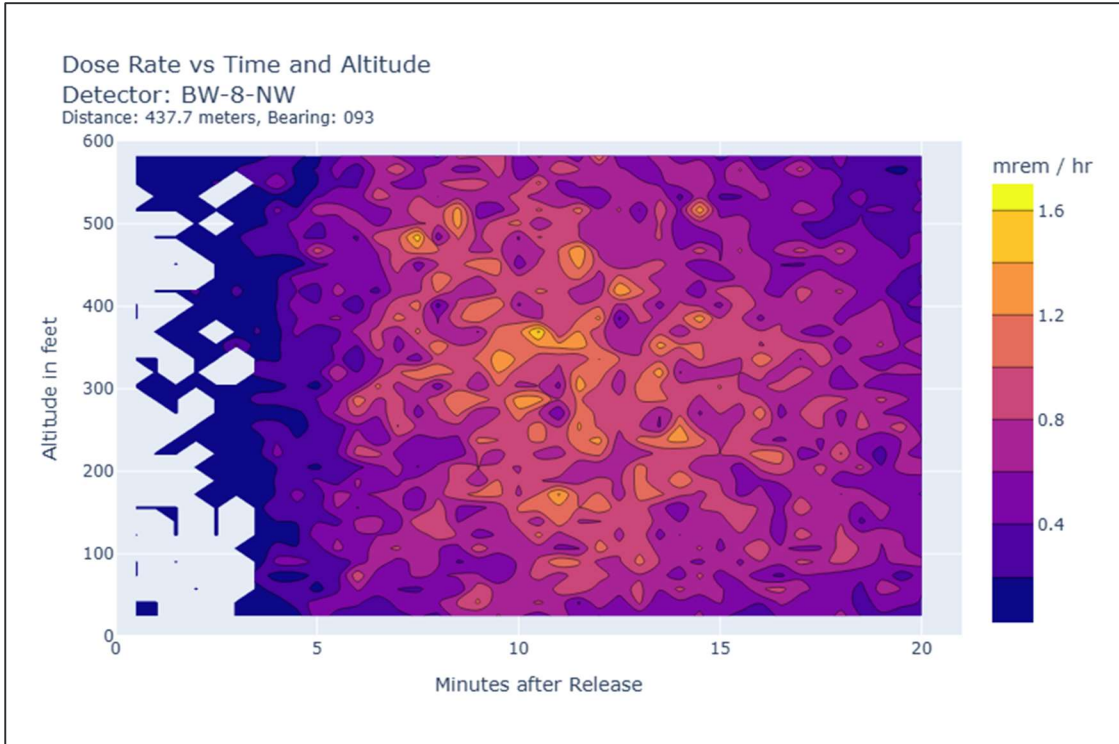


Figure 5.7. Dose rate over time of detector BW-8-NW

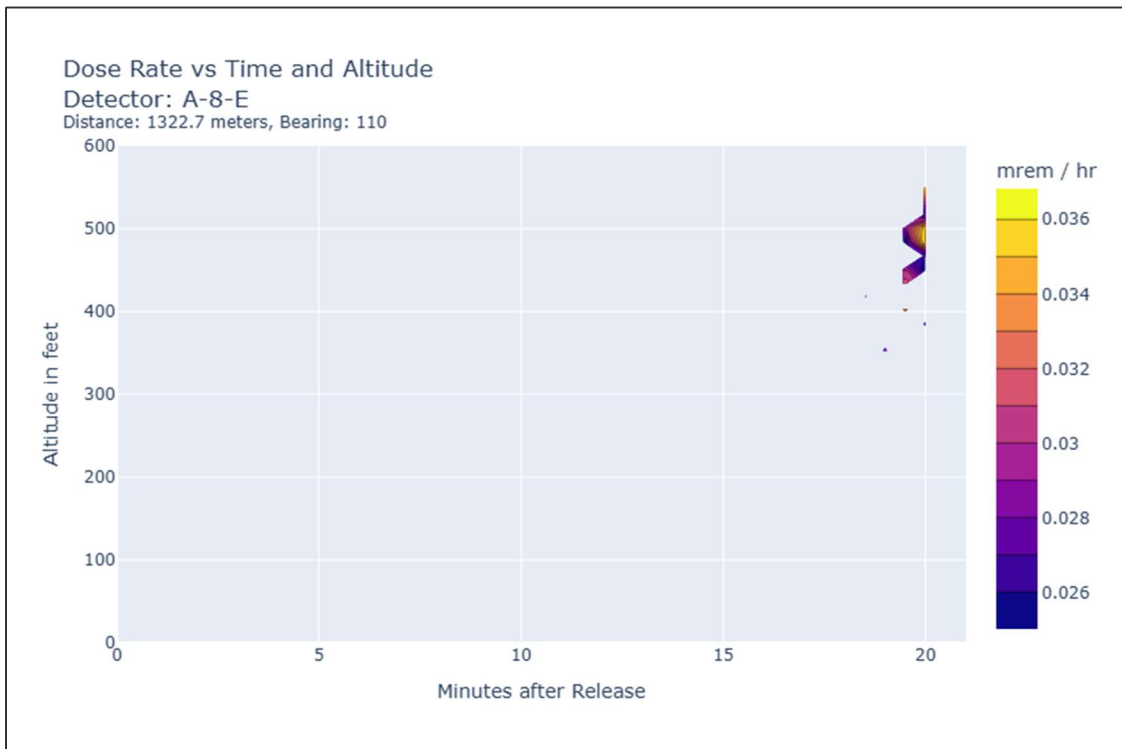


Figure 5.8. Dose rate over time of detector A-8-E

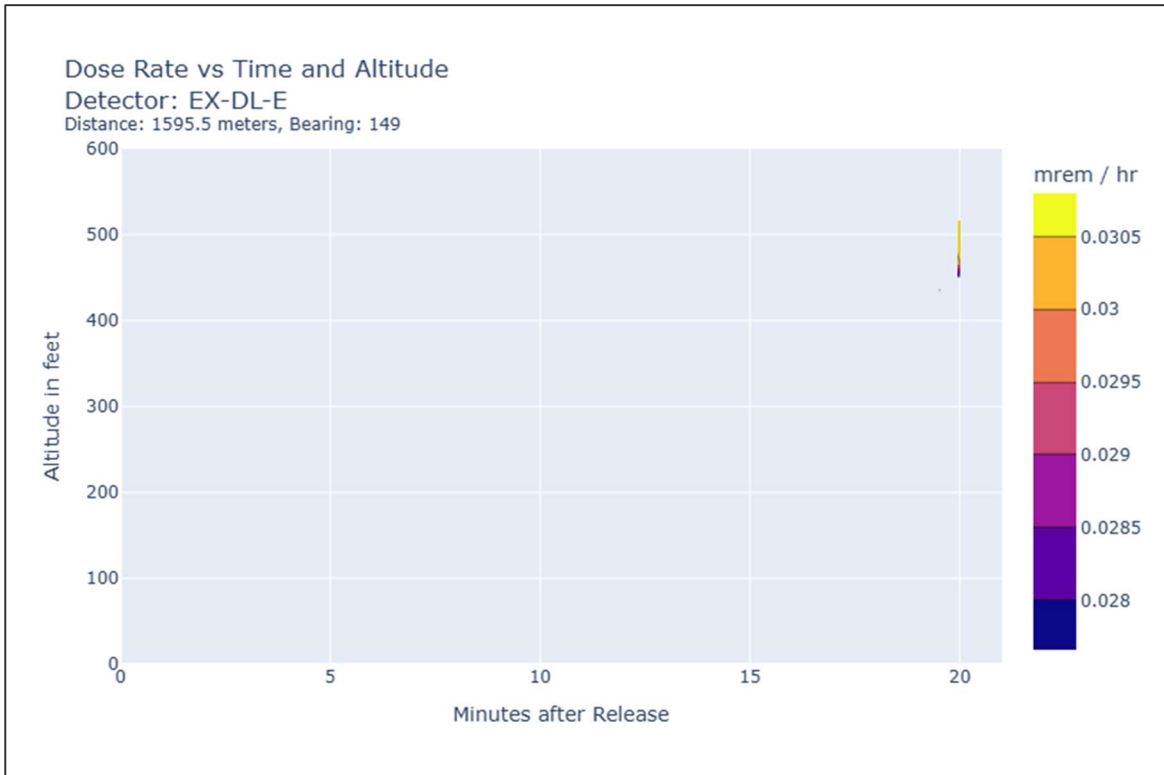


Figure 5.9. Dose rate over time of detector EX-DL-E

Note that while the horizontal and vertical axes ranges are held constant in Figure 5.7 through Figure 5.9 (and on all dose rate plots in this section), the color scale varies between figures.

This configuration could get multiple detections within 20 minutes if the detectors could be placed at altitudes of 137 meters or greater. Most buildings in this section of Manhattan are 10 stories or less, making such placement impractical.

Table 5-3. Evaluation of alternative four-detector configuration with 1 km spacing

Criteria	Results
Event Detection	Yes 0.025 to 0.15 mrem / hour at ground level
Event Confirmation	No Only one detector
Time to Detection	1 minutes at multiple heights 3 minutes at ground level
Release Location	No data from sensor system Based on wind direction, to the west Distance unknown
Plume Direction	No data from sensor system Based on wind direction, to the east
Dose Rate Boundaries (10 R / hr, 10 mr / hr)	No data from sensor system
Dose Estimates (5R, 1R in first 4 days)	Sensor system is not helpful At least 10 mrem at ground level (assuming 0.1 mrem / hr), but no indication of worst-case dose rate

## 5.7 Half Kilometer Spacing

We next evaluated the performance of a system of 22 detectors with an approximate spacing of a half kilometer. Due to how we selected monitoring locations, the spacing between adjacent detectors ranges from 400 to 500 meters (Figure 5.10).

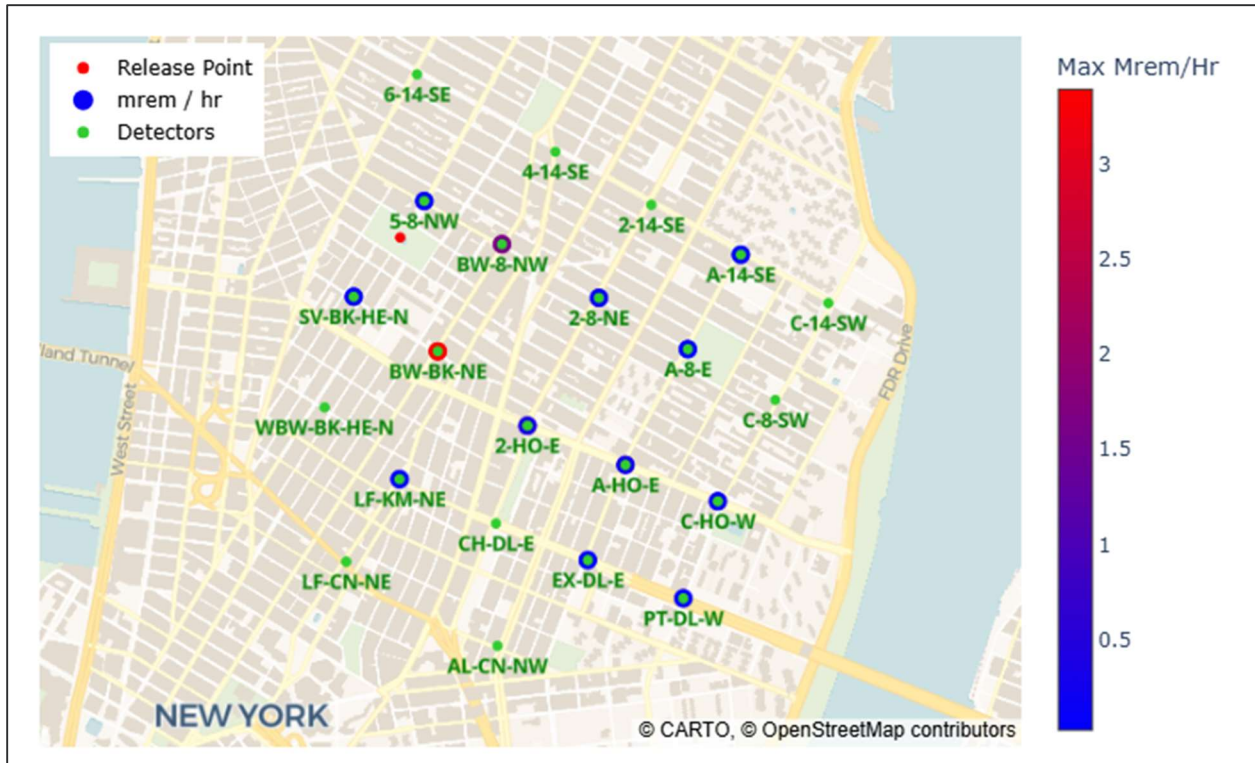


Figure 5.10. Configuration of 22 detectors equally spaced 400 to 500 meters apart

We observed dose rates above 0.025 mrem / hour on thirteen of the 22 detectors. Detectors A-14-SE, PT-DL-W, and LF-KM-NE were elevated for less than a minute, so they are not counted as possible detections.

The following section reviews dose rate versus time and altitude for the nine possible detections, by distance from the release point.

### 5.7.1 Dose Rates

The closest detection occurred 186 meters from the release point. Elevated dose rates were apparent near ground level between 5 and 12 minutes after the release (Figure 5.11). The next closest monitoring location was 320 meters southwest of the release point. However elevated dose rates were apparent only above 91 meters, which exceeds the height of most structures in this area (Figure 5.12). The first persistent detection near ground level occurs at Broadway and 8<sup>th</sup> Avenue (BW-8-NW), 440 meters from the release point (Figure 5.13). The next three detector locations show persistent detections at ground level (Figure 5.14 through Figure 5.16). Only one of the remaining four detectors (A-HO-E, Figure 5.18) has a persistent detection near ground level.

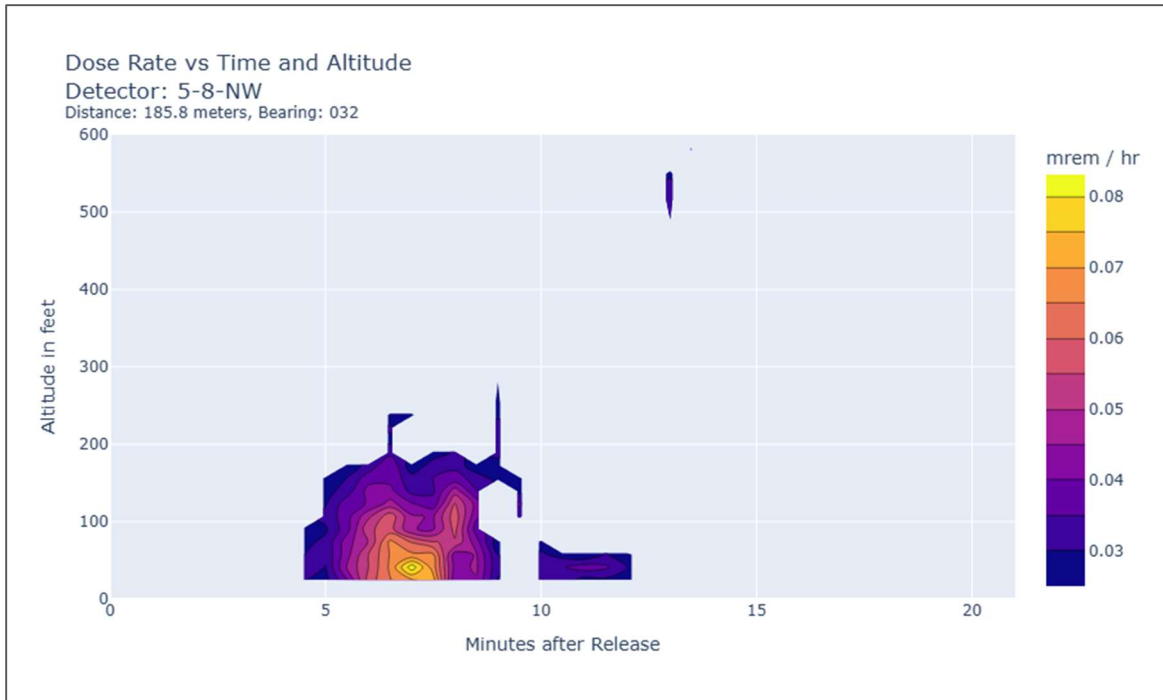


Figure 5.11. Dose rate over time of detector 5-8-NW

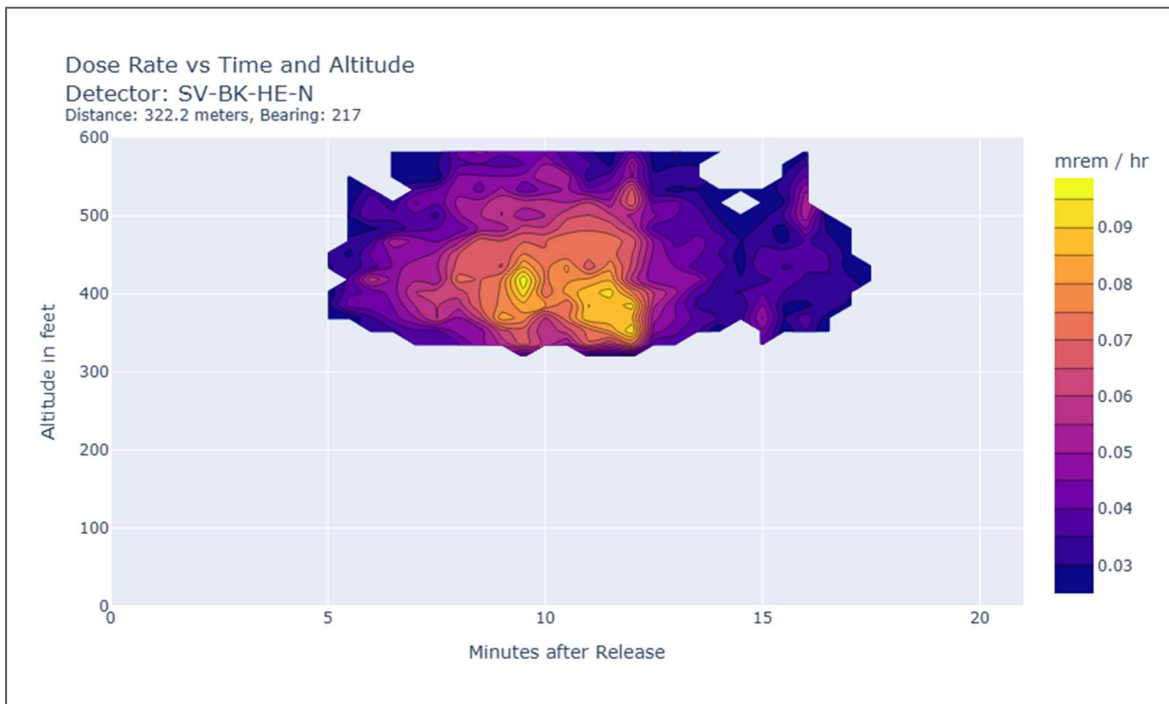


Figure 5.12. Dose rate over time of detector SV-BK-HE-N

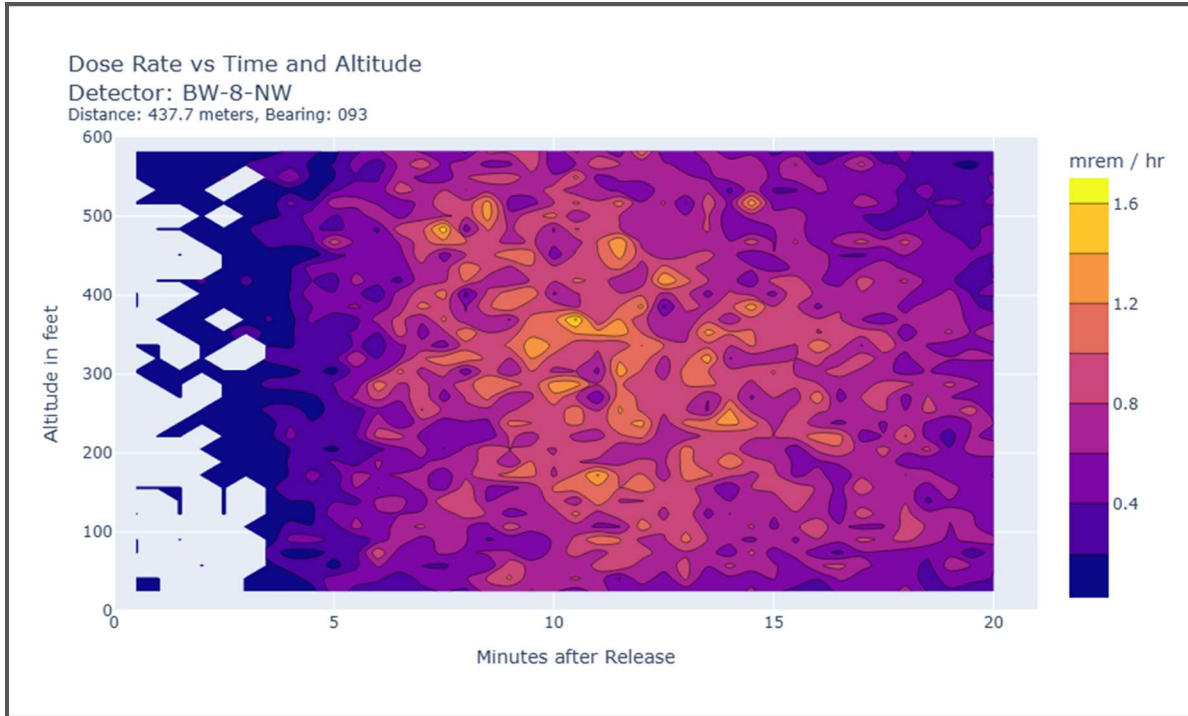


Figure 5.13. Dose rate over time of detector BW-8-NW

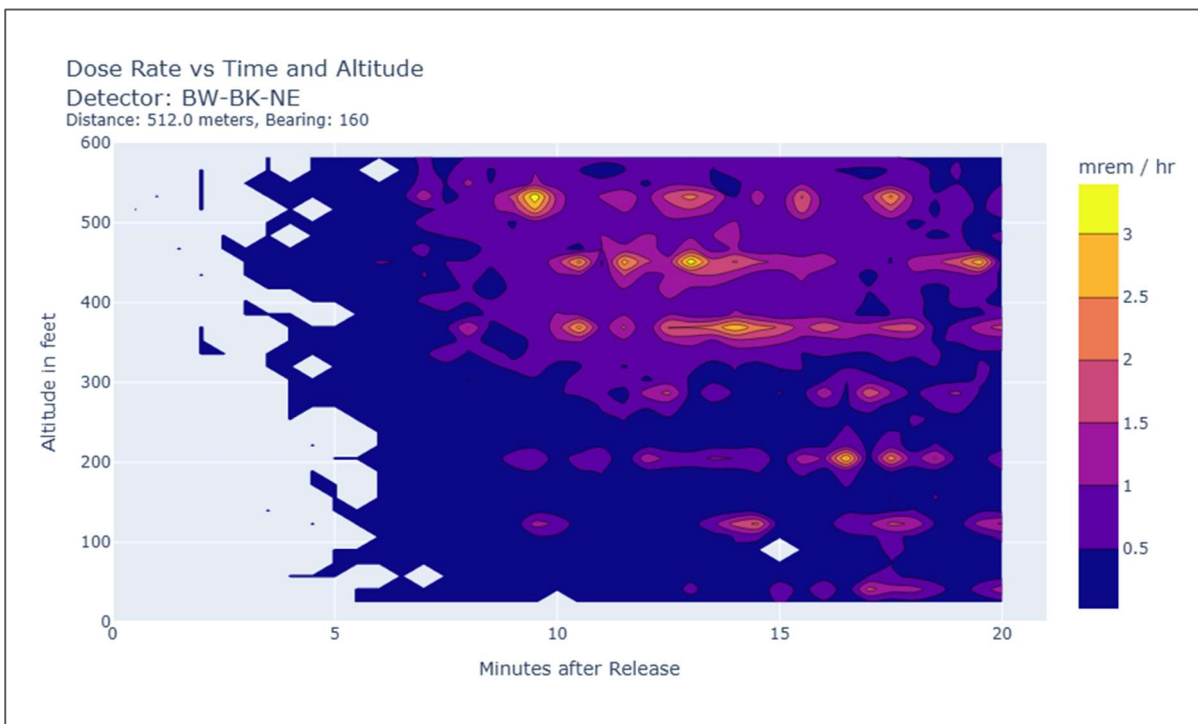


Figure 5.14. Dose rate over time of detector BW-BK-NE

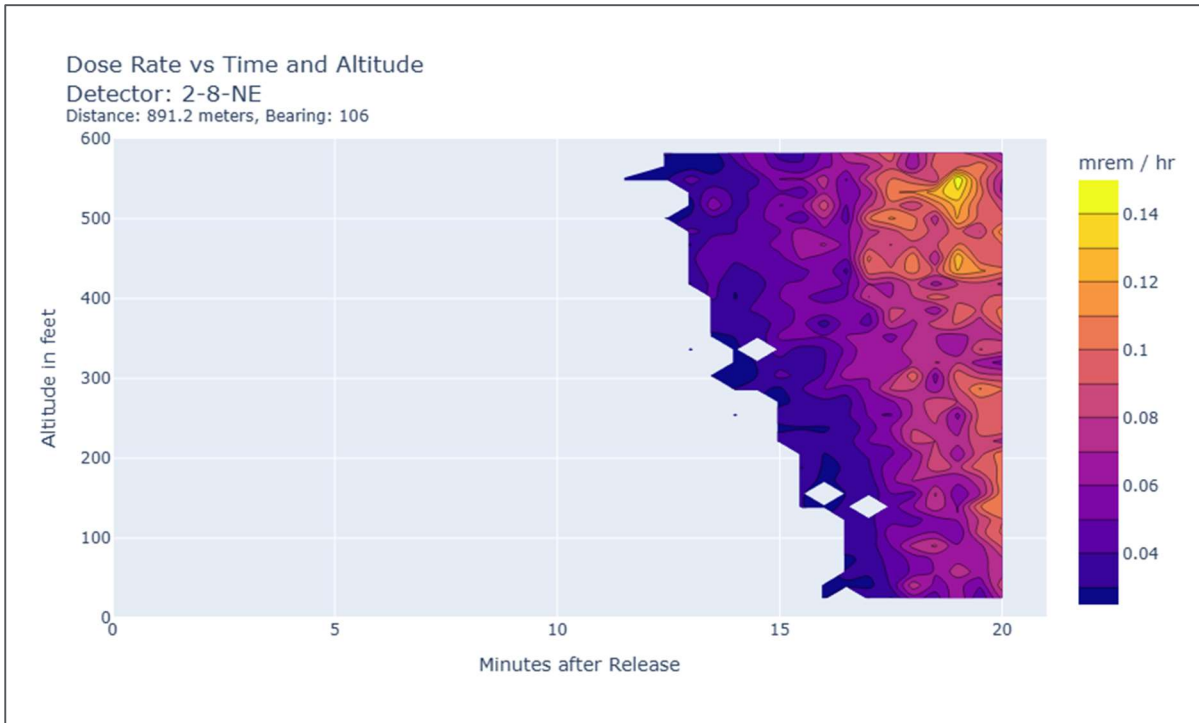


Figure 5.15. Dose rate over time of detector 2-8-NE

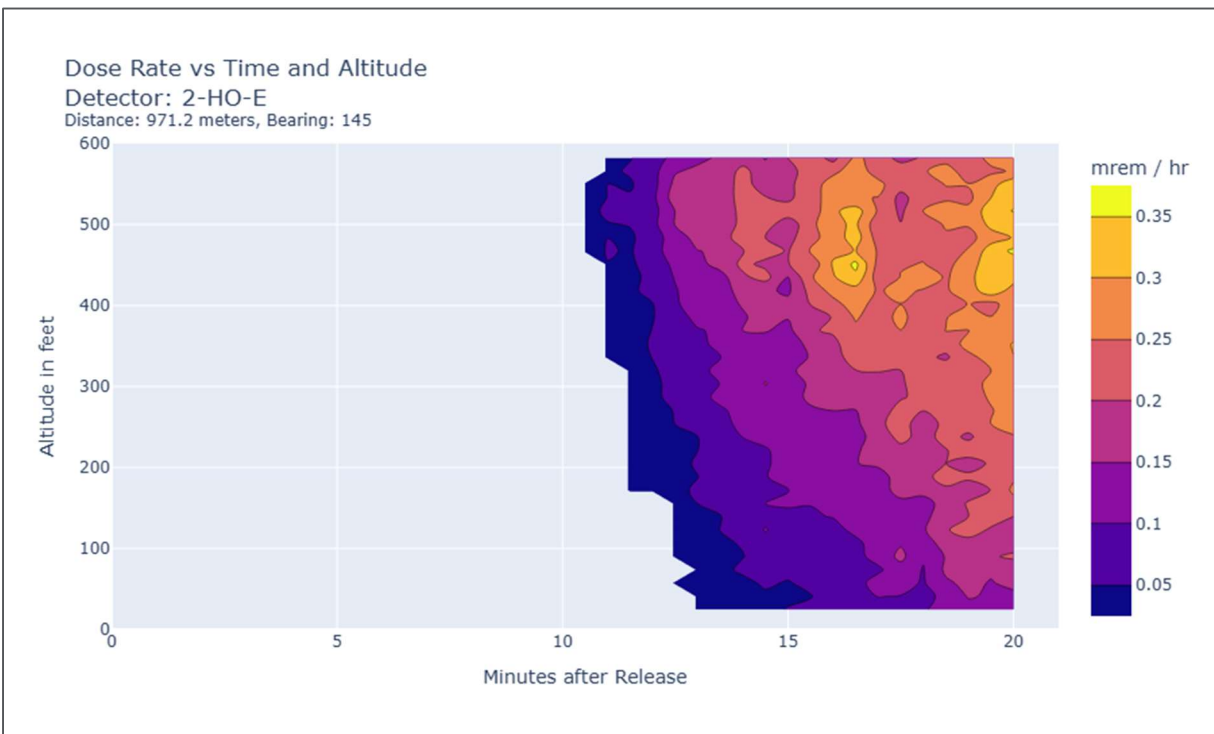


Figure 5.16. Dose rate over time of detector 2-HO-E

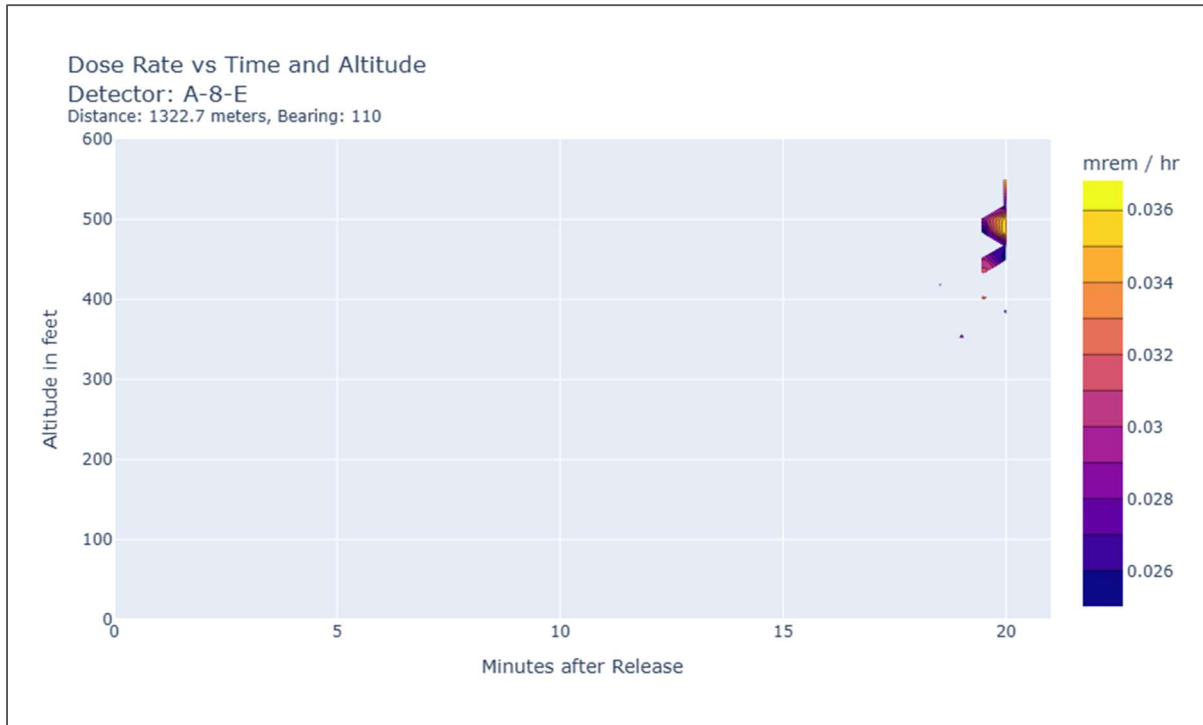


Figure 5.17. Dose rate over time of detector A-8-E

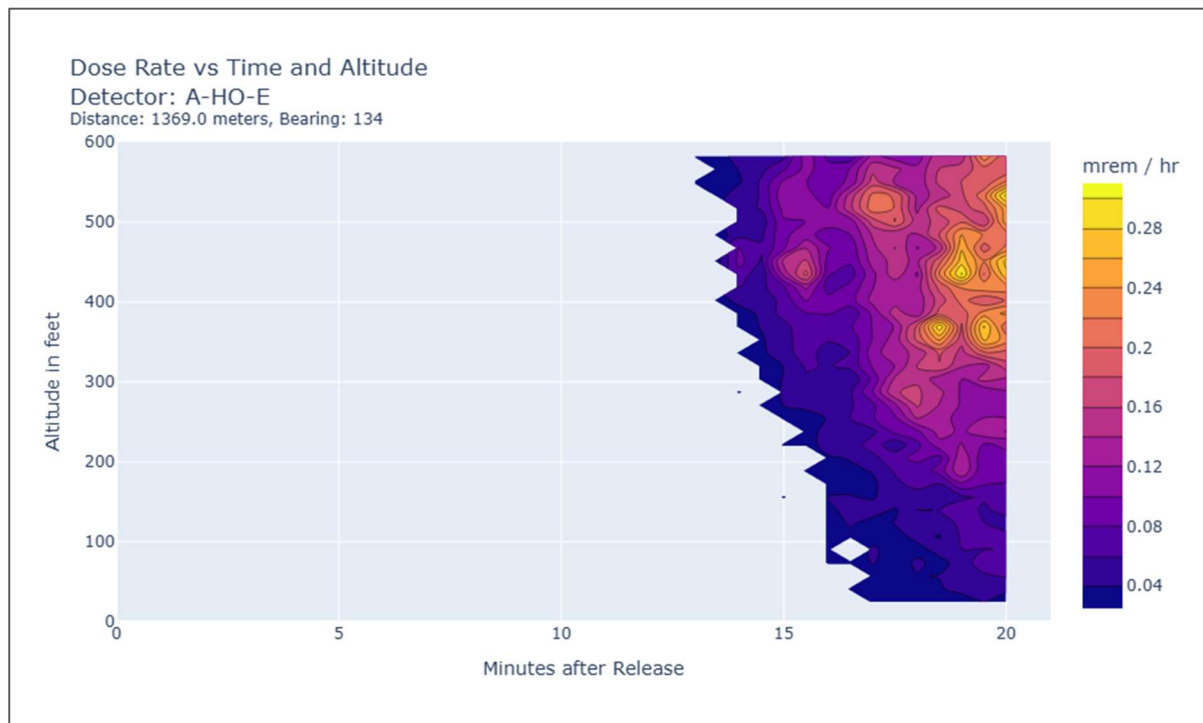


Figure 5.18. Dose rate over time of detector A-HO-E

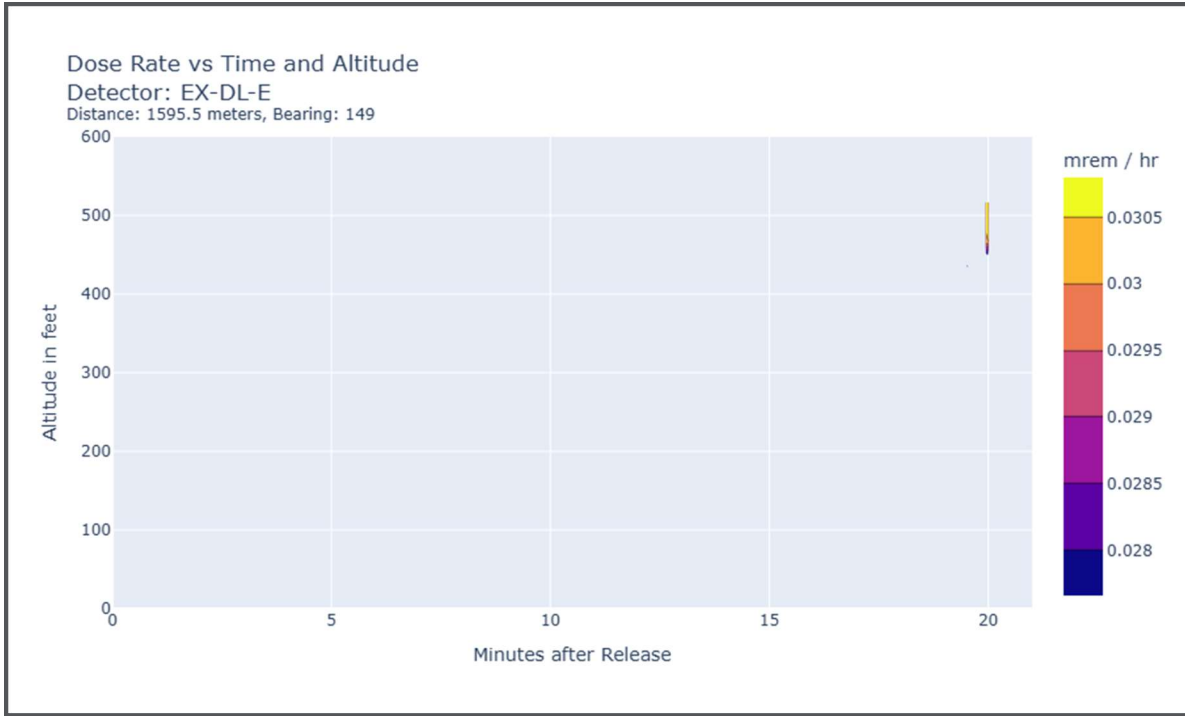


Figure 5.19. Dose rate over time of detector EX-DL-E

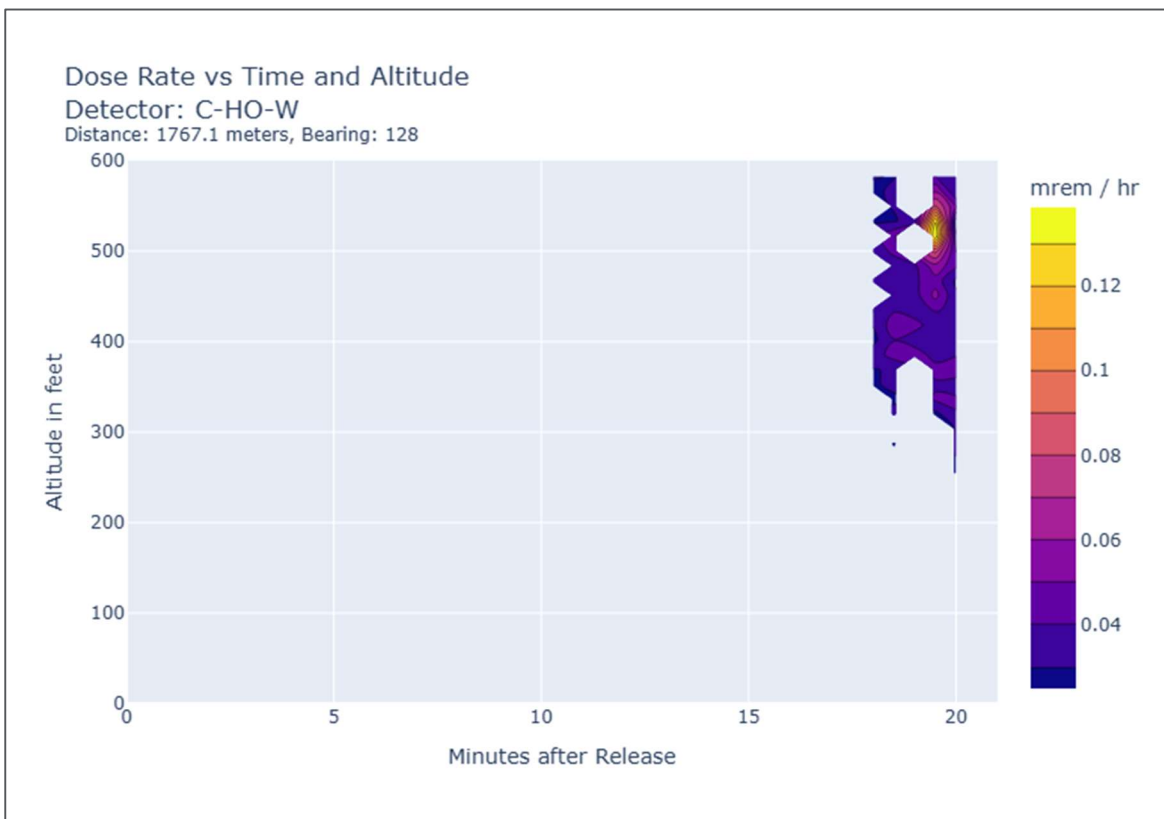


Figure 5.20. Dose rate over time of detector C-HO-W

Unsurprisingly, detectors further from the release point take longer to detect elevated dose rates. Figure 5.21 shows the time to detection where there were persistent detections near ground level. Table 5-4 shows how the 500-meter sensor configuration performed relative to our evaluation criteria.

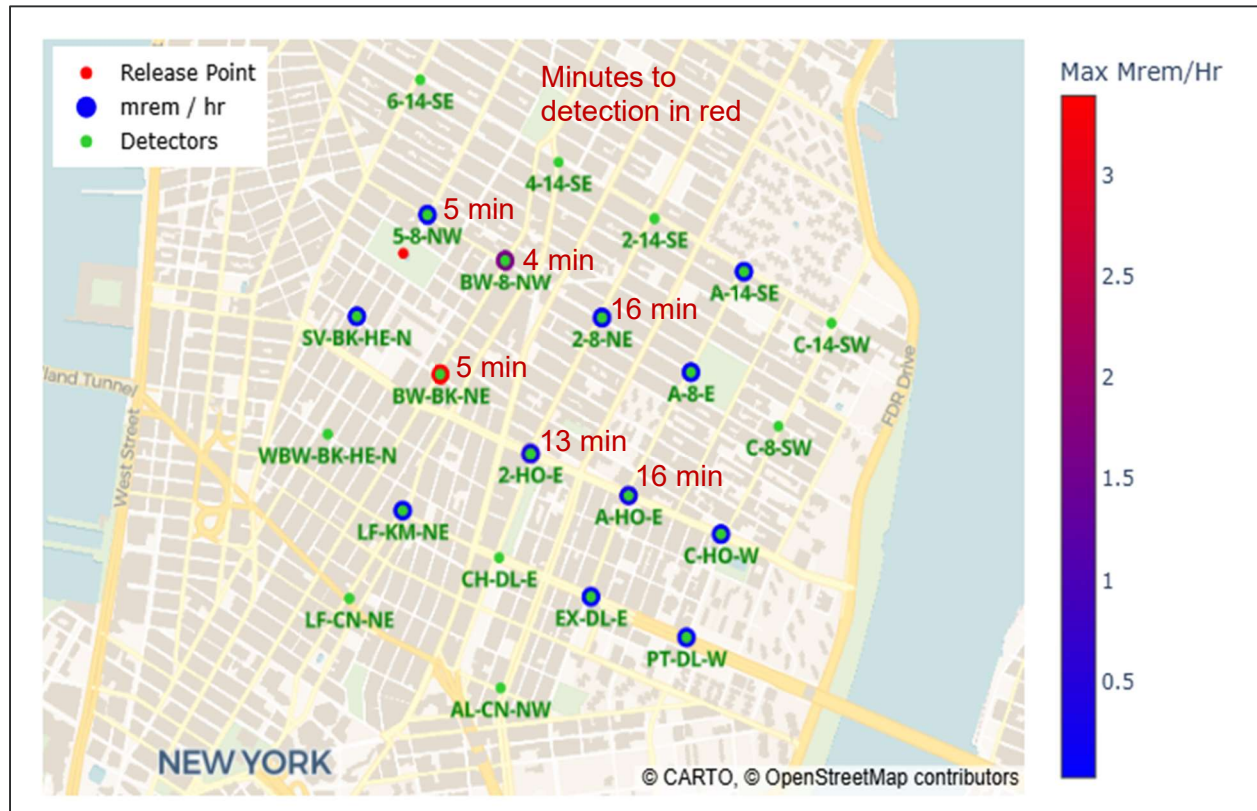


Figure 5.21. Time for a detector location to observe an activity above 0.25 mrem/hr at ground level

Table 5-4. Does a detector configuration with 500-meter spacing meet the evaluation criteria

Criteria	Results
Event Detection	Yes
Event Confirmation	Yes, persistent detection on multiple detectors rules out detector fault or localized anomaly
Time to Detection	4 - 5 minutes at ground level
Release Location	Between 4th and 6th avenues, 8th and Houston streets, wind direction could further narrow release location
Plume Direction	Clear that plume is moving west to east
Dose Rate Boundaries (10 R / hr, 10 mr / hr)	Indeterminate, max dose rate from detectors at ground level is 0.5 mrem / hr. Maybe could estimate max dose rate with distance attenuation calculations?
Dose Estimates (5R, 1R in first 4 days)	Indeterminate. At least 50 mrem at ground level (assuming 0.5 mrem / hr)

## 5.8 Analysis Based on Activity Levels

In addition to analyzing dose rates, we attempted to estimate detector response using only the concentration of Cs-137 particles that were generated by the QUIC model. This technique does not estimate dose rates for a given location, but it has the advantage of not requiring time-consuming dose rate calculations for every possible detector location.

To understand the impact of the location of sensors on the detectability of a plume, the placement methods described in Section 3.1 were applied to different timepoints of plume passage. The methodology generally assumed that the determined activities surrounding each placed sensor represented the sensor response. This allows a sensor agnostic approach to be implemented during this portion of the review.

### 5.8.1 Number of Sensors

Determining the number of sensors is a calculation of budget divided by cost per unit. This defines the numbers of sensors that are available for the layout. This starting point impacts the number of sensor locations that should be considered for placement. The examples provided in Section 5.0 use 25 sensor locations and are for descriptive purposes only. A complete discussion of the impact of changing the number of sensors can be observed by reading the entirety of this section.

### 5.8.2 Planar Layouts

Planar layouts assume that the sensors are placed at a uniform height above ground. They were reviewed at heights of 0, 12.5 and 37.5 meters. This portion of the review used all three

placement method types described in Section 3.1 to analyze the impact of uniform height on plume detectability. The sensor locations are displayed in Figure 5.22 through Figure 5.25.

The designation of sensor placement locations for assessed in Table 5-5 through Table

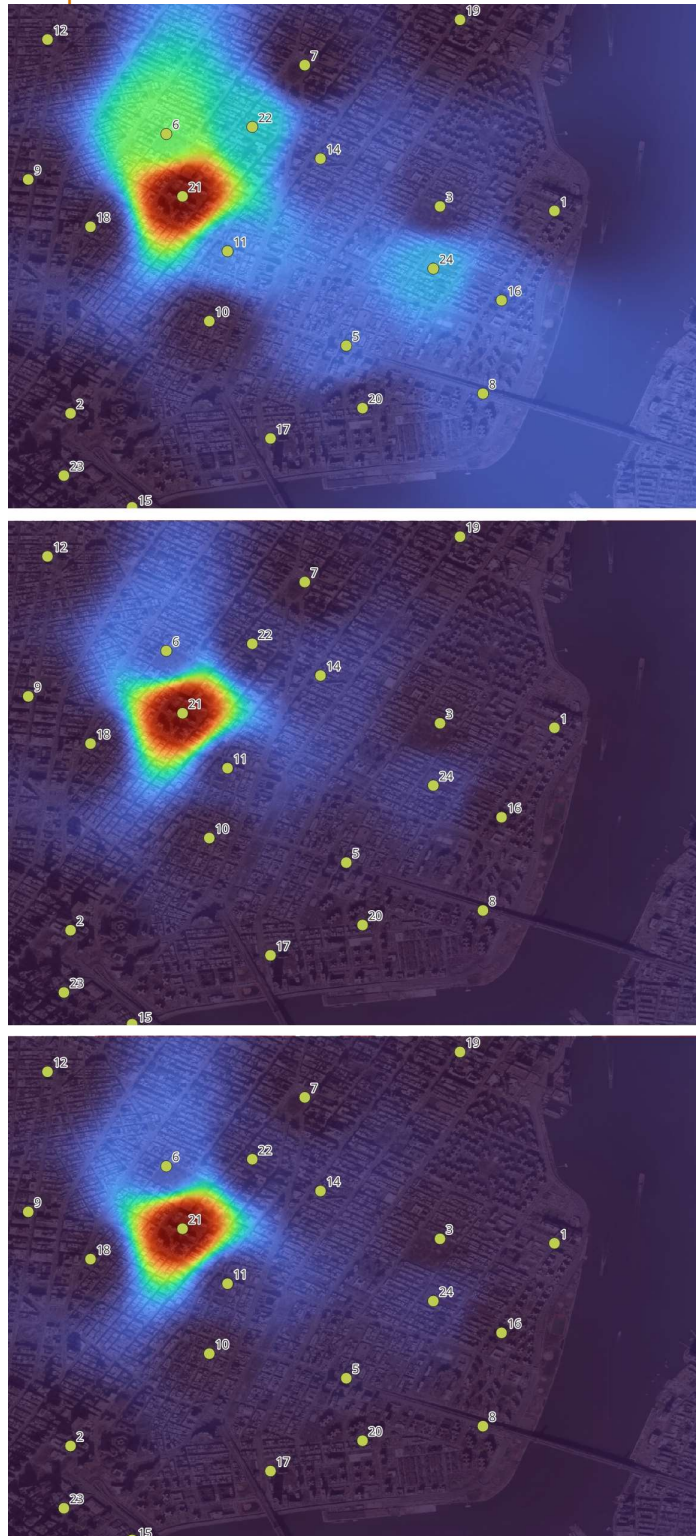


Figure 5.24. Random Sensor Placement, Ground Level, 41.5 Minutes after Release, At ground level (top), 12.5 meters (middle) and 37.5 meters (bottom)

Table 5-7 was completed using Visual Sample Plan (VSP) (Matzke et. al., 2014). The color scale shows what activity levels would be calculated by VSP if Kriging were used. Kriging is a statistical interpolation technique used in geostatistics and other fields for spatial data analysis. The Kriging algorithm is estimating the activity levels at locations where there are no detectors.

Figure 5.22 through Figure 5.25 bear little resemblance to figure the simulated Cs-137 distribution that is plotted in Figure 4.7. These differences suggest that Kriging does not accurately estimate the geographic extent of radioactive contamination in this scenario. This is unsurprising in retrospect because at least 30 data points are recommended for Kriging (Matzke et. al., 2014).

The placement strategies are assessed in Table 5-5 through

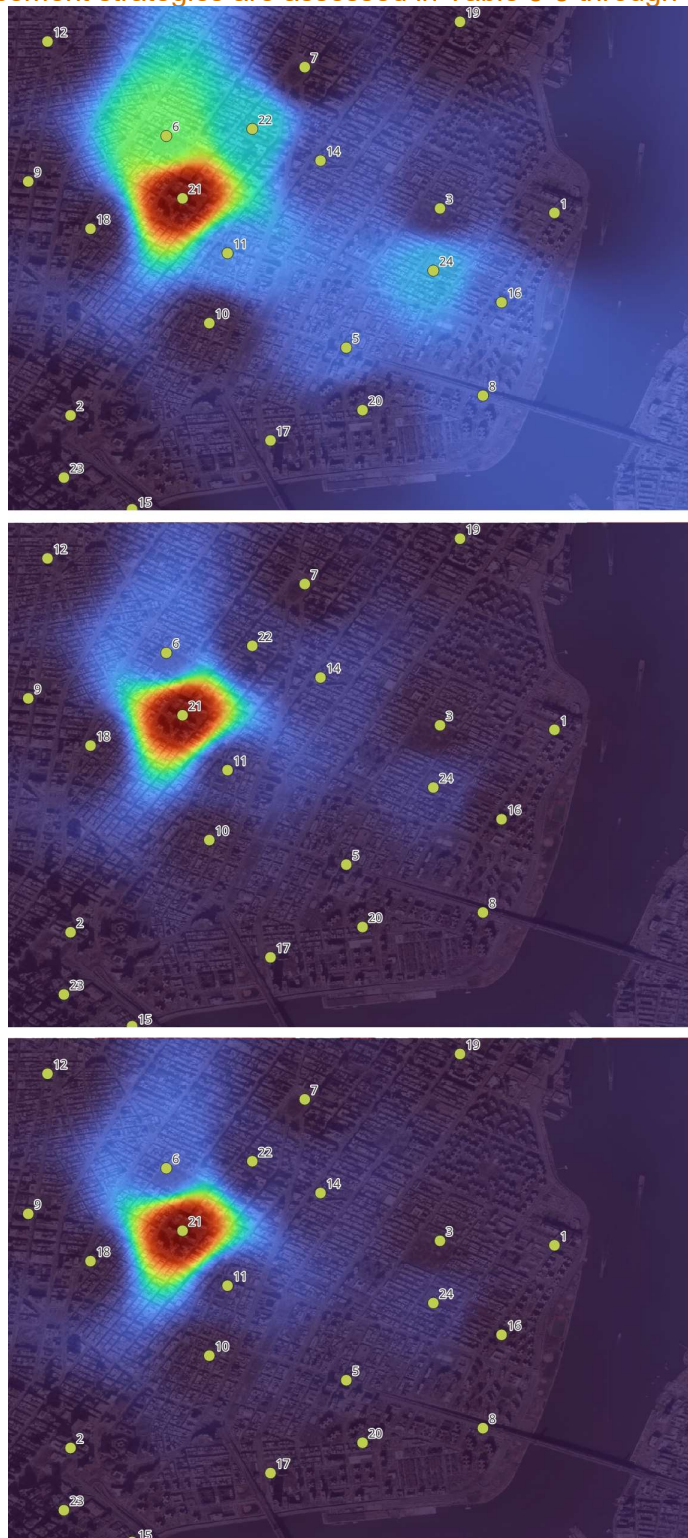


Figure 5.24. Random Sensor Placement, Ground Level, 41.5 Minutes after Release, At ground level (top), 12.5 meters (middle) and 37.5 meters (bottom)

Table 5-7. Due to the time required to calculate dose rates, the planar sensor layouts were analyzed using activity levels (equivalent to the concentration of Cs-137 particles). Our analysis assumes that 60,000 or more disintegrations per minute would result in a detectable dose rate. The DHS RDD response guidance (DHS, 2017) recommends placing areas that exceed 60,000 dpm within the hot-zone boundary. Note that disintegrations per minute (DPM) is different than counts per minute (CPM). DPM refers to the actual number of decays that are occurring in the radioactive material that is being measured. CPM refers to the decays that are counted by the detector. CPM will be less than DPM. The relationship between DPM and CPM depends on the detector's geometry and efficiency.



Figure 5.22. Systematic Sensor Placement, Ground Level, 41.5 Minutes after Release, At ground level (top), 12.5 meters (middle) and 37.5 meters (bottom)

Table 5-5. Systematic Sensor Placement

Criteria		Results
Event Detection	Yes	
Event Confirmation	Yes, persistent detection on multiple detectors rules out detector fault or localized anomaly	
Time to Detection	4 - 5 minutes at ground level	
Release Location	Between 4th and 6th avenues, 8th and Houston streets, wind direction could further narrow release location	
Plume Direction	Clear that plume is moving west to east	
Dose Rate Boundaries	Yes, multiple detectors surpass hot zone guidance activity	
Dose Estimates (5R, 1R in first 4 days)	Indeterminate.	

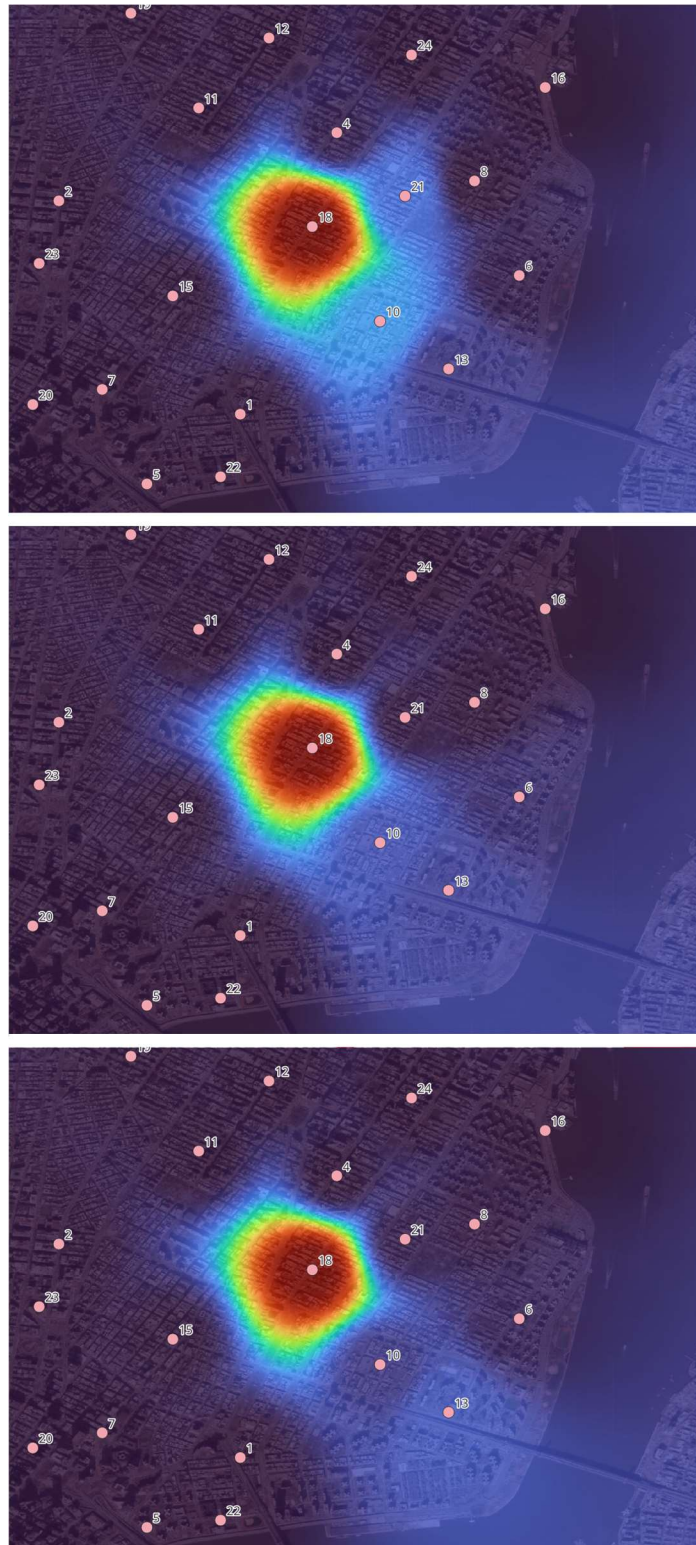


Figure 5.23. Random Sensor Placement, Ground Level, 41.5 Minutes after Release, At ground level (top), 12.5 meters (middle) and 37.5 meters (bottom)

Table 5-6. Random Sensor Placement

Criteria	Results
Event Detection	Yes
Event Confirmation	Yes, persistent detection on multiple detectors rules out detector fault or localized anomaly
Time to Detection	4–5 minutes at ground level
Release Location	At or west of randomly placed detector 18
Plume Direction	Clear that plume is moving west to east
Dose Rate Boundaries	Yes, multiple detectors surpass hot zone guidance activity
Dose Estimates (5R, 1R in first 4 days)	Indeterminate.

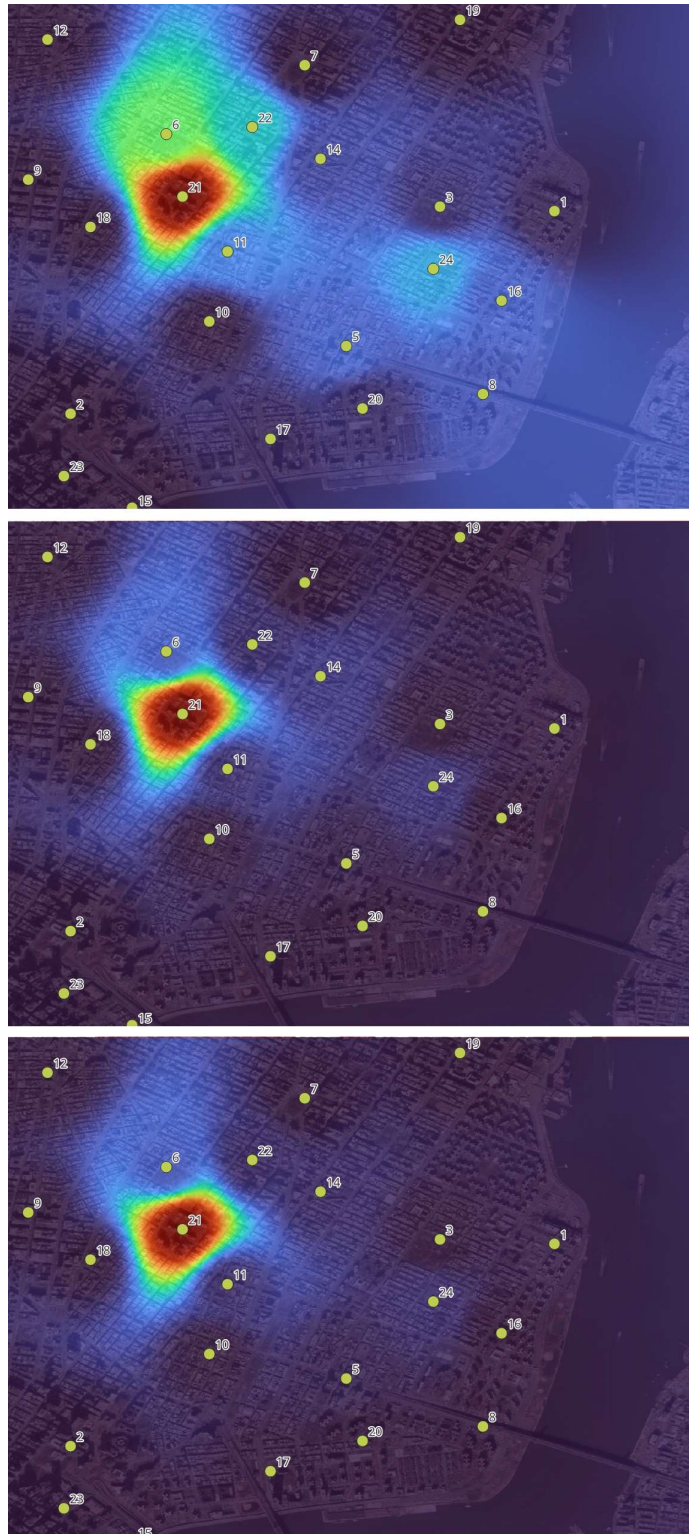


Figure 5.24. Random Sensor Placement, Ground Level, 41.5 Minutes after Release, At ground level (top), 12.5 meters (middle) and 37.5 meters (bottom)

Table 5-7. Random Placement, Alternate Configuration

Criteria	Results
Event Detection	Yes
Event Confirmation	Yes, persistent detection on multiple detectors rules out detector fault or localized anomaly
Time to Detection	4 - 5 minutes at ground level
Release Location	At or near Alternate Randomly placed Sensor 21
Plume Direction	Clear that plume is moving west to east
Dose Rate Boundaries	Yes, multiple detectors surpass hot zone guidance activity
Dose Estimates (5R, 1R in first 4 days)	Indeterminate.



Figure 5.25. Fire stations and Police Precincts, Ground Level, 41.5 Minutes after Release, At ground level (top), 12.5 meters (middle) and 37.5 meters (bottom)

Finally, a strategic placement method used existing responder locations as a basis for locations of sensor placement was evaluated (**Error! Not a valid bookmark self-reference.**).

Table 5-8. Sensors Placed at Fire Stations and Police Precincts

Criteria	Results
Event Detection	Yes
Event Confirmation	Yes, persistent detection on multiple detectors rules out detector fault or localized anomaly
Time to Detection	4 - 5 minutes at ground level
Release Location	At or near FDNY Engine 33/Ladder 9 engine houses
Plume Direction	Clear that plume is moving west to east
Dose Rate Boundaries	Yes, multiple detectors surpass hot zone guidance activity
Dose Estimates (5R, 1R in first 4 days)	Indeterminate.

## 6.0 Recommendations

It is important to note that this report analyzed a limited number of detector configurations for a single RDD scenario. The analysts who generated this report knew the location of the release point when they selected the dose rate monitoring locations. Therefore, it's not clear if the trends observed in this analysis will be relevant for other scenarios in different geographic locations and in other weather conditions. Nevertheless, this section includes some general recommendations for detector placement.

### 6.1 Detector Spacing

If possible, we recommend a detector spacing of 500 meters or less. For the modeled scenario (releasing 1000 Ci of Cs-137), a detector configuration with spacings greater than 1 kilometer might miss the RDD release entirely. The analysis also suggests that configurations with detector spacings of 500 meters or less are likely to detect the release of radioactive material on multiple detectors. However, a system with 500 meters spacing could be prohibitively expensive to install, monitor, and maintain. A ten-by-ten kilometer area would require 121 detectors.

Detector systems with larger than 500-meter spacing might still be effective for releases significantly larger than 1,000 Ci, however our analysis shows that a 1,000 Ci release still has significant radiological consequences. For comparison, the blood irradiator that was the source of the 2019 Harborview release contained a total of 2,900 Ci of Cs-137, and only a small fraction of the 2,900 Ci was released (NNSA, 2020).

### 6.2 Detector Altitude

We recommend installing a portion of the detectors at higher altitudes (100 – 150 meters) if the geographic region of interest has structures that are sufficiently tall and suitable for mounting radiation monitoring equipment. The remaining detectors can be placed near ground level. Detectors near well-known locations that might be targets for RDDs should also be at ground level (or at the same altitude as the target).

At distances greater than 400 meters from the release point, the highest dose rates and earliest detections tended to occur at higher altitudes. This result is consistent with the vertical distribution of Cs-137 activity. Figure 6.1 shows a plot of Cs-137 activity 12 minutes after the release. The color scale represents the altitude that has the highest concentration of Cs-137 (red). The highest activity levels occur at lower altitudes near the release point, and at higher altitudes farther from the release point. We suspect that higher-altitude Cs-137 particles are traveling faster because wind speeds are greater at higher altitudes. It's also possible that buildings could be blocking or slowing the dispersion of particles at lower altitudes.

We were not able to run sufficient simulations to determine the optimal ratio of high-altitude to ground-level detectors. In practice, we expect that this ratio would be determined by the quantity and distribution of tall structures that are suitable for mounting. We suspect there are benefits to having at least half the detectors near ground level. We expect more activity to deposit near ground level and that ground-level dose rates are more relevant for estimating personnel exposure.

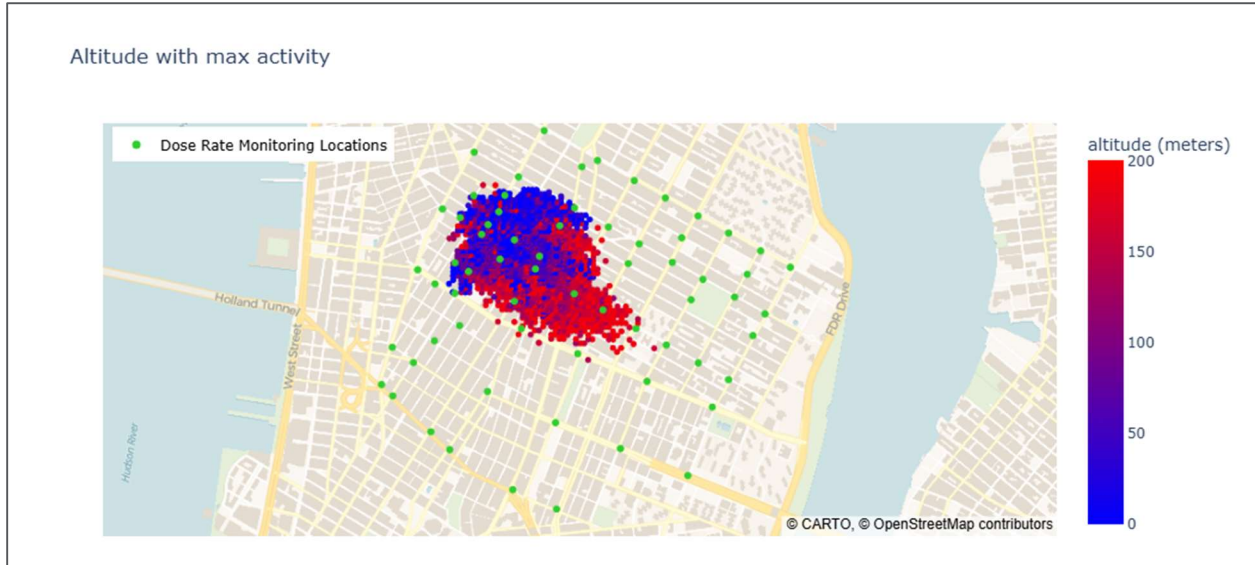


Figure 6.1. Cs-137 plot 12 minutes after release

### 6.3 Kriging Analysis

We recommend against using Kriging analysis during the early phases of an incident, unless there are detections from at least 30 detectors spread over the region of interest. We found that with a limited number of detectors, Kriging does not produce accurate results.

Figure 6.2 shows the results of using Kriging to estimate dose rates for the 1-kilometer scenario described in Section 5.5. The highest estimated dose rates are in the dark red areas and the lowest dose rates are in the dark blue areas. Kriging erroneously suggests that the highest dose rates are in the northeast quadrant of our simulation area, and that there is little or no radiation exposure at the release point. Kriging does better as we add more detectors. Figure 6.3 shows how Kriging performs with detectors at a 500-meter spacing. Kriging does better with 500-meter spacing, correctly identifying the area with the highest dose rates. However, it provides no indication of plume direction.

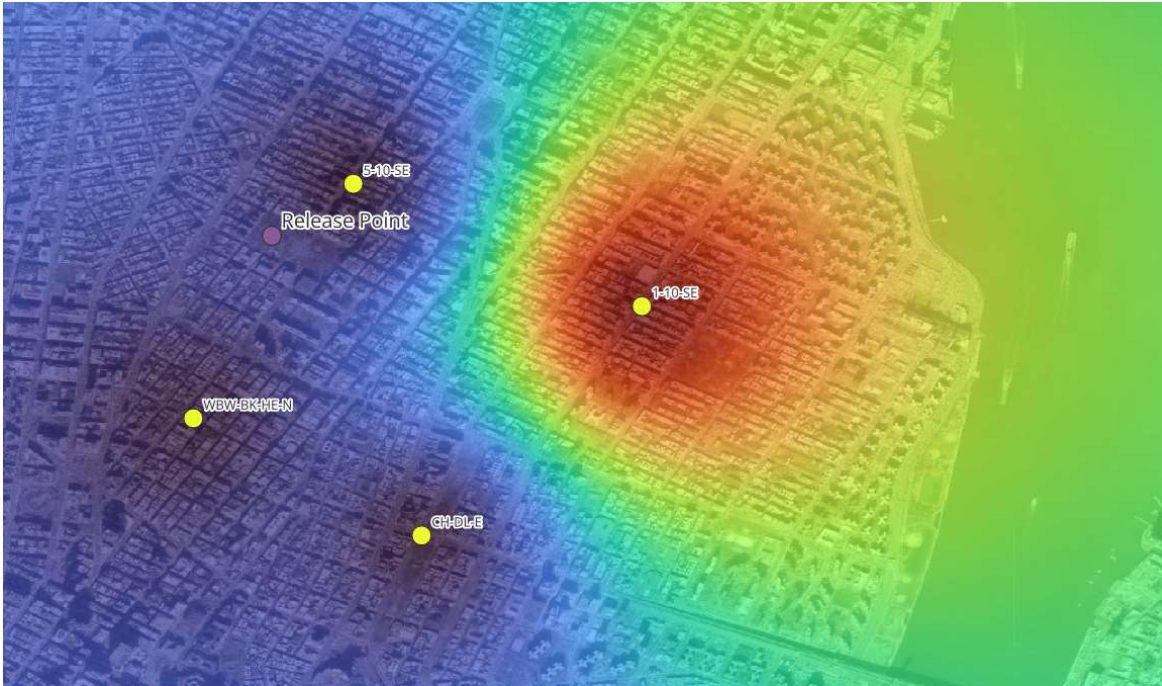


Figure 6.2. Kriging Analysis Using Four Detectors



Figure 6.3. Kriging Analysis Using 500-Meter Detector Spacing

## 6.4 General Sensor Guidance

So far, our recommendations only addressed detector spacing and altitude. There are many other considerations for emergency planners who are considering installation of fixed position sensor systems.

1. The geographic area that will be monitored,
2. Selection of sensors to be used for monitoring,
3. Number of sensors available to the organization, and
4. Ability to place sensors within the area to be monitored.
5. Upper bounding of sensors

Sensor selection considerations include:

- Sensor selection must meet the organizational needs that are described in Section 2.5 of this document.
- A sensor must be able to detect the contaminant(s) of concern.
- A sensor must have a response range that:
  - Encompasses activities very close to natural background.
  - Includes levels that could be observed during a dispersal event.
- A sensor must be capable of supplying data that can be actively monitored.
- A sensor must be able to alarm or alert users to radiation events that exceed thresholds of notification.
- The sensor must be rugged enough to survive in the monitored area.
- A detector that is non-functional due to environmental concerns is no more useful than not having one.

The number of sensors available will impact the organization's ability to reach a sensor density that increases the likelihood to identify and, depending on the characteristics of the selected sensor, characterize a dispersal event. As shown in Section 5.0 increasing the sensor density increases the likelihood of detection. However, it also demonstrated that the ability to bound a plumes direction may also provide beneficial information. The closest spacing reviewed in during this project was 400 to 500 meters. This density provided sufficient detail to identify and bound the plume for the scenario studied.

Additional methodology on the ability to place sensors and availability of continued access to the placement location was considered in Section 5.0. Random, systematic, and strategic sampling can each provide benefits to some extent. For smaller jurisdictions, the strategic placement of detectors at locations of first responders is recommended. This will allow sensors to be placed at locations with continued access for general maintenance of the instruments. It will likely also provide additional benefit of go/no go indications at those responder locations during an event. Jurisdictions that incorporate response minimization techniques for city planning will likely also minimize distance between sensors.

The sensor should also be able to identify radioactive material deposition at or near ground level based on its placement above ground. This will provide continued monitoring of the current conditions at a location, but also provide responders with situational awareness guidance for the conditions at or near the sensor location.

We recommend against the random placement of sensors for any jurisdiction. This approach could result in large areas being unmonitored or receiving limited monitoring, which outweighs any benefits from eliminating placement bias.

## 7.0 Conclusion

Our simulations and analysis demonstrated that the WRF, QUIC, and MCNP models can be combined to simulate releases of radioactive materials in urban environments. We did encounter limitations on the size of the geographic area and the number of buildings that can be simulated. Nevertheless, we were able to simulate an RDD event and evaluate the performance of simple detector systems.

Our analysis generated suggestions related to placement and spacing for systems of fixed sensors. However, our analysis focused on a single isotope and a single geographic location. We do not know to what extent these results will apply in different weather conditions or in other locations with different urban densities.

We recommend that additional research be conducted in this area. Developing guidelines for the design of radiation detection systems will require analysis of more scenarios that cover a wide range of locations, isotopes, activity levels, and weather conditions. Refer to *Sensor Placement Optimization Study for the Built Environment: Next Steps Report* (PNNL, 2025) for more detailed information on potential improvements to the modeling framework and additional analysis that would improve our understanding of how radioactive plumes interact with built environments.

This page intentionally left blank.

## 8.0 References

Abate, S. R. (2015). Smart inverter settings for improving distribution feeder performance. *2015 IEEE Power & Energy Society General Meeting*, (pp. 1-5). Denver

Brodsky, A., and R.G. Gallagher. "Statistical Considerations in Practical Contamination Monitoring," *Radiation Protection Management* 8 (4):64-78. July/ August 1991.

Currie, L.A. "Limits for Qualitative Detection and Quantitative Determination," *Analytical Chemistry* 40(3):586-593. 1968.

Department of Homeland Security (DHS). 2017. *Radiological Dispersal Device (RDD) Response Guidance*. [https://www.dhs.gov/sites/default/files/publications/nustl\\_rdd-responseplanningguidance-public\\_28oct2021-508-revised.pdf](https://www.dhs.gov/sites/default/files/publications/nustl_rdd-responseplanningguidance-public_28oct2021-508-revised.pdf)

ICRP. (2010). Conversion Coefficients for Radiological Protection Quantities fro External Radiation Exposures. ICRP Publication 116. *Ann. ICRP*, 40, 2-5.

Kulesza, J. A., Adams, T. R., Armstrong, J. C., Bolding, S. R., Brown, F. B., Bull, J. S., . . . McKinn, G. W. (2022). *MCNP Code Version 6.3.0 Theory & User Manual*. Los Alamos National Laboratory, Los Alamos, NM, USA.

Matzke B. D., Wilson J.E., Newburn L. L., Dowson S. T., Hathaway J. E., Sego L. H., Bramer L. M., Pulsipher B. A. (2014). *Visual Sample Plan Version 7.0 User's Guide*. PNNL-23211. Pacific Northwest National Laboratory. <https://vsp.pnnl.gov/docs/PNNL%2019915.pdf>

Metwally, W., Gardner, R. P., & Sood, A. (2004). Gaussian broadening of MCNP pulse height spectra. *Transactions of the American Nuclear Society*, 91, 789-790.

Multi-Agency. 2023. *Interagency Agreement (IA) Between DHS Science & Technology Directorate and the DOE Pacific Northwest National Laboratory 70RSAT23KPM000034 Statement of Work (SOW)*.

Nelson, M., & Brown, M. (2013). *The Quick Urban & Industrial Complex (QUIC) Dispersion Modeling System*. Los Alamos National Laboratory, Los Alamos, NM, USA.

National Nuclear Security Administration (NNSA). *Sealed Source Recovery at the University of Washington Harborview Training and Research Facility Results in Release of Cesium-137 on May 2, 2019*. <https://www.energy.gov/sites/prod/files/2020/04/f73/JIT-Seattle-Cesium-Event-2019-05-02.pdf>

*NCRP 58. A Handbook of Radioactivity Measurements Procedures*. Bethesda, Md.: National Council on Radiation Protection and Measurements. February 1, 1985.

Proctor, A. (2020). Deconvolving plastic scintillator gamma-ray spectra using particle Swarm optimization. *IEEE Nuclear Science Symposium and Medical Imaging Conference*. IEEE.

Pacific Northwest National Laboratory (PNNL). 2025. *Sensor Placement Optimization Study for the Built Environment: Next Steps Report*.

Skamarock, W. C., J. B. Klemp, J. Dudhia, D. O. Gill, Z. Liu, J. Berner, W. Wang, J. G. Powers, M. G. Duda, D. M. Barker, and X.-Y. Huang (2019). A Description of the Advanced Research WRF Version 4. *NCAR Tech. Note NCAR/TN-556+STR*.

<https://opensky.ucar.edu/islandora/object/technotes%3A576>

U.S. Environmental Protection Agency (EPA). 2017. *PAG Manual: Protective Action Guides and Planning Guidance for Radiological Incidents*. EPA-400/R-17/001

[https://www.epa.gov/sites/default/files/2017-01/documents/epa\\_pag\\_manual\\_final\\_revisions\\_01-11-2017\\_cover\\_disclaimer\\_8.pdf](https://www.epa.gov/sites/default/files/2017-01/documents/epa_pag_manual_final_revisions_01-11-2017_cover_disclaimer_8.pdf)

U.S. Environmental Protection Agency (EPA). 2025. *RadNet Dashboard*.

<https://www.epa.gov/radnet/radnet-near-real-time-air-data>.

This page intentionally left blank.

## Appendix A – Modeling Methodology

The Quick Urban and Industrial Complex (QUIC) dispersion modeling system (Nelson & Brown, 2013) combines three-dimensional wind field modeling with atmospheric transport simulations heavily adapted to the peculiarities of urban environments to produce a relatively portable, building-aware model of airborne particulate movement over time scales on the order of hours. QUIC allowed significant flexibility in defining the size, extent, composition, time, and location of the particle release event while also drastically reducing the amount of effort required to model existing urban environments by supporting the import of ESRI ShapeFiles. QUIC's cohesion with other components of the modeling toolchain used in this work was another motivator behind its inclusion, as the software natively supported the capability to output time-dependent airborne particle location data in the format of an MCNP input file.

The Monte Carlo N-Particle (MCNP) transport code (Kulesza, et al., 2022) was used to model the transport of radiation from airborne and deposited radioactive particulates in the aftermath of an incident. Specifically, the built environments and locations of airborne and deposited particles were utilized to create a simulated geometry of the system; this geometry was fed to MCNP, which mapped the particle flux and imparted dose rate from the radioactive particles present on a 5x5x5 m grid overlaid on the geometry. In addition, high-fidelity simulations of detector energy response were carried out in the analysis of detector placement strategies.

Upon acquiring the necessary ShapeFile corresponding to the geographical region under consideration, the simulated city geometry was imported into QUIC using its city generator tool. Memory constraints limited the geographical area available within a single simulation to 2 km in each direction (assuming all buildings were at most 200 m tall with footprint areas of at least 45 m<sup>2</sup>) with a resolution of 25 m per side, producing an 80 x 80 x 8 voxel grid on which ShapeFile building objects were overlaid. This grid was then translated and rotated according to the region's Universal Transverse Mercator (UTM) projection encoded within the ShapeFile's metadata. The resulting highly detailed set of building geometries were then saved for use within QUIC, while a simplified version of this geometry (replacing complex building shapes with transformed rectangular prisms) was saved separately to facilitate the creation of a corresponding geometry capable of conforming to MCNP's rigid geometry definition rules; while QUIC includes native functionality intended to export geometries in a computer-aided design (CAD) format compatible with MCNP, these capabilities were inoperative in the version of the software used for this work (6.4.7), requiring the development of an alternative geometry translation methodology.

Following the execution of QUIC-URB and QUIC-PLUME, the locations of all source particles at each time point were exported to MCNP-formatted text files. From these source position files, and the building location data found in QUIC's corresponding geometry definition file, all of the necessary information could be gathered to create a fully defined recreation of each individual time point during plume transport within MCNP. To reduce the computational load of importing the full ~3.2 km<sup>3</sup> geometry (of which the plume particles likely occupied only a small percentage at any given time) for each of these simulations, the bounds for each simulation were set to encompass all of the plume particles present at that time point (with a 5 m buffer in each direction) with any building locations outside of this area ignored for that time point; reference to geographical location was maintained by using UTM position information to place MCNP building objects. Within these bounds, individual simulations were further limited to a maximum of 500 buildings apiece: geometries exceeding this limit were split into multiple simulations and

their results were concatenated in post-processing. Buildings were defined with uniform material compositions and densities (concrete at a density of  $2.3 \text{ g/cm}^3$  was chosen for the results presented in this work), while particle locations were represented as a distribution of point sources; the energy distribution of source particle emissions was determined based on isotopes present and their relative abundances.

One million independent particle histories, sampling from the provided position and energy distributions, were simulated to map (on a  $5 \times 5 \times 5 \text{ m}$  grid) the approximate gamma-ray flux due to the plume at a given point in time; these results were then transformed separately to create two output data streams. One stream merely involved separating the gridded flux results into equally-spaced bins based on the energy of contributing gamma-rays, while the other utilized a pointwise energy-dependent function to translate fluxes into corresponding dose rates in units of rem/hr; chosen function values were obtained from the isotropic (ISO) flux-to-dose conversion factors provided in Table A.1 of the International Commission on Radiological Protection's (ICRP) Publication 116 (ICRP, 2010) (converted from units of pSv/s to the desired rem/hr).

Example results from the MCNP QT Plotter are shown in at two different elevations at 30 s in Figure A.1, where the color scale is rem/s in each  $5 \times 5 \times 5 \text{ m}^3$  voxel, varying many orders of magnitude. In this scenario, the highest dose rate was 1.27 rem/hr close to the release point at ground level and quickly falls off to  $< \text{mrem/hr}$  levels within  $\sim 100 \text{ m}$ . The buildings clearly show shielding effects from the highest dose-rate regions. The white regions in the figures are areas where there was little or no radioactive material. As such, they are low-sampled regions in the MCNP radiation transport simulation (and likely at background dose rate levels).

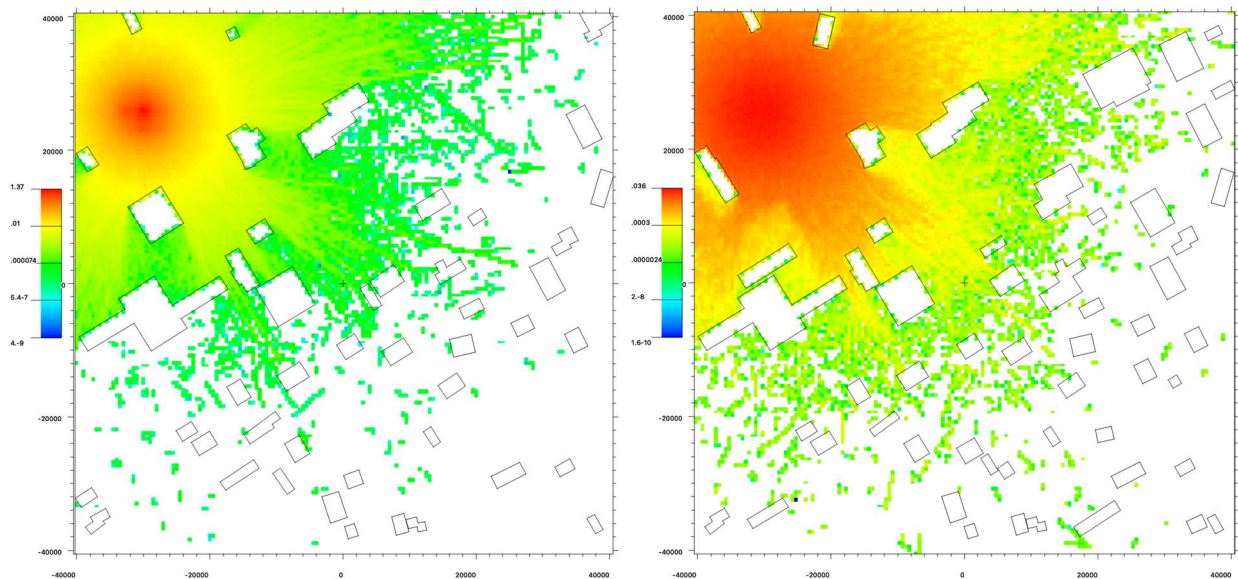


Figure A.1. Top-down views of the MCNP-computed dose rates from a plume dispersion at 30 s at 0.1 m (left) and 90 m (right) elevation above ground.

Energy binned flux results were then employed in another MCNP-based model of the anticipated detector responses to the plume at various geographical locations. To estimate the total gamma-ray flux incident on a given detector, the energy-binned flux map was translated into a source term with a detector placed in a random grid cell; the contributions from each nearby grid cell were then mapped (radiating outward until the relative flux contribution was less than 1/1,000,000 of the total) and binned in energy. This process was then repeated using additional randomized grid cells until the relative flux contributions within each cell converged. The energy binned flux results from the original MCNP simulation were then convolved with these flux contributions to produce the gamma-ray flux spectrum incident on a detector at a specified location, which was then subsequently used in simulating the detector response at that location. Simulated detector responses for energy-discriminating instruments were adjusted to approximate the statistical fluctuations that produce imperfect detector energy resolution using MCNP's Gaussian energy broadening capability, with function input coefficients for NaI (TI) (Metwally, Gardner, & Sood, 2004) and polyvinyl toluene (PVT) (Proctor, 2020) scintillators obtained from literature.

## Appendix B – Minimum Detectable Activity

This guidance applies to instruments that report dose rates and to instruments that report count rates. Dose rate information has an additional conversion applied to gross count rates to provide an estimate of the dose rate at that location at that time. This is usually limited to instruments that measure beta and gamma radiation. When measuring at or near background dose rates, instruments are frequently paired with data loggers to watch trends over time. This allows for identification of spatial or temporal patterns during review.

The relationship between background and MDA is a mathematical function of the current background activity at the time. This relationship is described in detail in NUREG-1507 *Minimum Detectable Concentrations with Typical Radiation Survey Instruments for Various Contaminants and Field Conditions*. (NRC 1997). There are multiple methodologies that have been determined empirically and they are listed in Table B-1. The equations in this table are focused on count rate instruments that report total counts over time. This instrument is considered more sensitive to radioactivity levels at or very close to natural background.

Table B-1. Minimum Detectable Activity calculation methods from NUREG-1507

Mathematical Expression	Reference
$2.71 + 4.65 * \sqrt{B}$	NCRP 58 / EPA 1980
$2.71 + 4.65 * \sqrt{B}$	Currie 1968
$3 + 4.65 * \sqrt{B}$	Brodsky & Gallagher 1991
$\frac{3 + 3.29 * \sqrt{R_b t_g \left(1 + \frac{t_g}{t_b}\right)}}{Efficiency * t_g}$	Strom & Stansbury 1992 <sup>1</sup>

Generally, all of the equations listed in Table B-1 will supply a similar answer, but these equations are targeted at activities that are very close or similar to natural background and can be applied to all types of radiation. The identification of background should be represented by the typical response shown by a sensor at a location.

The US EPA operations a national network of more than 200 radiation monitoring stations within the US called the RadNet<sup>2</sup>. The monitoring stations in this network provide ambient air monitoring for each location. Certain locations provide additional monitoring of precipitation and/or drinking water. These can be used to identify generic baseline conditions for most locations, though site-specific data is always preferable for location specific comparisons.

<sup>1</sup>The terms *B*, *R<sub>b</sub>*, *t<sub>B</sub>*, and *t<sub>g</sub>* refer to background counts, background counting rate, gross count time, and background counting time, respectively. Using *t<sub>B</sub>* equal to *t<sub>g</sub>* (1 minute), resulted in the same expression as that of Brodsky and Gallagher (1991).

<sup>2</sup> <https://www.epa.gov/radnet>

## Thresholds of Detection

There are two primary methods for establishing a numeric detection threshold. Detection thresholds can vary depending on current or recent background activity, or a constant threshold that's based on the highest expected background and desired false alarm rate can be established.

Variable thresholds of detection require constant monitoring of ambient radiation levels. It requires use of previously collected data to (count rate or dose rate per unit time) to compare against current conditions. This methodology can be resource intensive due to the constant need for data.

Constant thresholds are much simpler to apply. Setting constant thresholds requires knowledge instrument response characteristics and expected background radiation levels for the area where the detector is located. Depending on the data provided by the instrument, the detection threshold can be specified as a count rate (e.g., counts per minute) or a dose rate (e.g., mrem per hour).

Use of numeric thresholds provides a provides a reasonable likelihood of meeting the criteria for plume identification and potentially characterization. These thresholds should consider all the potential purposes for the instrument, but for the purpose of this guidance the primary purpose is identification and characterization of a plume. Ideally, detection thresholds will be set low enough to reduce the risk that a radiological event will be undetected, but high enough such that local responders do not become indifferent to false alarms and dull to response actions. There are many potential causes of false alarms, including industrial radiography, transport of radiopharmaceuticals, and passage of people who are being treated with medical isotopes.

To that end, numeric thresholds are published in the DHS RDD response guidance that can be considered for example purposes (DHS, 2017). The RDD response guidance recommends that areas with activity levels greater than 60,000 DPM (6,000 DPM if alpha contamination is present) or dose rates greater than 10 mrem per hour.

## Appendix C – Glossary

**Americium-241 (Am-241)** – A man-made isotope that emits alpha particles and a low-energy gamma ray. It has a half-life of 432 years and is commonly used in smoke detectors.

**Beryllium-9 (Be-9)** – Be-9 is the most abundant, naturally occurring isotope of Beryllium. It is stable but emits a neutron when it absorbs an alpha particle. Be-9 is commonly combined with Am-241 (which emits an alpha particle) to create a neutron source.

**Cesium-137 (Cs-137)** – A radioactive isotope that is a common fission product of uranium-235. Cs-137 has a half-life of 30 years and emits a beta particle and a low-energy gamma ray. It is commonly used to calibrate radiation instruments, for radiation therapy, and to irradiate materials.

**Geiger Mueller Detector** – An instrument for detecting ionizing radiation. Geiger Mueller detectors are relatively simple and inexpensive, but they do not measure the energy of the incident particle, nor do they distinguish between different radiation types. However, when properly calibrated, they provide a sufficiently accurate approximation of external exposure from gamma rays.

**Protective Action Guideline** – “A projected dose to an individual from a release of radioactive material at which a specific protective action to reduce or avoid that dose is recommended.” (EPA, 2017)

**Radiological Dispersal Device** – A device that is used by a malicious actor to spread radioactive material over a wide area. Such devices are often conceptualized as a conventional explosive device around which radioactive material is packed. Detonation of the conventional explosive disperses the radioactive material and lofts it into the air, which forms a plume that can be transported by wind currents. It is important to note that an RDD incident is not a nuclear detonation. In a nuclear detonation, the nuclear fission or fusion reaction is the primary source of explosive energy, whereas the in an RDD detonation, the conventional explosive is the primary source of explosive energy.

**Sodium Iodide Detector** – A type of scintillation detector that uses a sodium iodide crystal as the detection material. Scintillation detectors emit light when gamma rays interact with atoms in the scintillator material. Scintillation detectors can measure the energy of the incident gamma rays because the intensity of the light produced in the material is proportional to the energy of the gamma ray. The energy measurement helps to identify the source of the radiation.

## Appendix D – MCNP Dose Rate Monitoring Locations

The UTM coordinates listed in **Error! Reference source not found.** are for zone 18N.

Table D-1. Locations of determined dose rates during MCNP Modeling

Location ID	Latitude	Longitude	Description	UTM - Easting	UTM - Northing	Distance to Release Point (meters)	Bearing from Release Point
1-10-SE	40.72867	-73.9844	1st Avenue and E 10th St., SE corner	585767	4509133	1147.9	101
1-12-SW	40.73001	-73.9837	1st Avenue and E 12th St., SW corner	585822	4509282	1181.4	94
1-14-SE	40.7312	-73.9825	1st Ave and E 14th St., SE Corner	585919	4509416	1275.8	87
1-4-SE	40.72506	-73.987	1st Avenue and E 4th St., SE corner	585551	4508730	1110.6	125
2-10-SE	40.72968	-73.9867	2nd Avenue and E 10th St., SE corner	585564	4509242	929	97
2-14-SE	40.73218	-73.9849	2nd Ave and E 14th St., SE corner	585720	4509522	1086.5	82
2-4-SE	40.72608	-73.9893	2nd Avenue and E 4th St., SE corner	585349	4508841	882	126
2-8-NE	40.7286	-73.9875	2nd Avenue and 8th St. E, NE corner	585500	4509123	891.2	106
2-HO-E	40.72369	-73.9912	2nd Avenue and E Houston St., E median	585199	4508574	971.2	145
3-10-SE	40.7306	-73.989	3rd Avenue and E 10th St., SE corner	585376	4509342	732.6	92
3-14-SE	40.73313	-73.9871	3rd Ave and E 14th St., SE corner	585530	4509626	922	73
4-14-SE	40.73422	-73.9897	4th Ave and E. 4th St., SE corner	585305	4509744	759	60
5-10-SE	40.73333	-73.9954	5th Ave and W 10th St., SE corner	584827	4509639	324.5	34
5-14-SE	40.73585	-73.9936	5th Ave and W 13th St., SE corner	584980	4509921	644.5	31
5-8-NW	40.73233	-73.9964	5th Avenue and W 8th St., NW corner	584745	4509527	185.8	32
5-WSN-NE	40.73143	-73.9968	5th Avenue and Washington Square North, NE corner	584710	4509427	86.6	49
6-10-SE	40.73468	-73.9986	6th Ave and W 10th St., SE corner	584556	4509786	424.2	348
6-13-SE	40.73656	-73.9973	6th Ave and W 13th St., SE corner	584667	4509996	625.4	2
6-14-SE	40.73719	-73.9968	6th Ave and W 13th St., SE corner	584708	4510067	698.9	5
6-4-SE	40.73158	-74.0009	6th Avenue and W 6th St., SE corner	584368	4509440	284.5	284
6-BR-SW	40.72404	-74.0045	6th Avenue and W. Broome St., SE corner	584072	4508600	960	216
6-CN-NE	40.72202	-74.0053	6th Avenue and W Canal St., NE corner	584010	4508374	1181.5	212

Location ID	Latitude	Longitude	Description	UTM - Easting	UTM - Northing	Distance to Release Point (meters)	Bearing from Release Point
6-HO-E	40.72827	-74.0027	6th Avenue and W Houston St., East side median	584221	4509071	518.6	234
A-10-SE	40.72775	-73.9822	Avenue A and E 10th St., SE corner	585954	4509033	1352.9	104
A-14-SE	40.73027	-73.9803	Avenue A and E 14th St., SE Corner	586106	4509314	1463.1	92
A-4-SE	40.72417	-73.9848	Avenue A and E 4th St., SE corner	585736	4508633	1318	124
A-8-E	40.72663	-73.983	Avenue A and E. 8th St., E side	585883	4508908	1322.7	110
A-HO-E	40.72219	-73.9862	Avenue A and E. Houston St., E median	585621	4508412	1369	134
AL-CN-NW	40.71523	-73.9927	Allen St. and Canal St., NW corner	585081	4507633	1792.1	165
B-10-SE	40.72678	-73.9799	Avenue B and E 10th St., SE corner	586148	4508928	1567.9	106
B-12	40.72803	-73.979	Avenue B and E 12th St., SE corner	586223	4509067	1608	100
B-14-SE	40.7293	-73.978	Avenue B and E 14th St., SE Corner	586302	4509209	1665.9	95
B-4-SE	40.72319	-73.9825	Avenue B and E 4th St, SE corner	585932	4508527	1539.9	123
BO-4-SE	40.72696	-73.9914	Bowery and E 4th St., SE corner	585173	4508936	684.9	129
BO-MB-NE	40.71628	-73.9958	Bowery and Manhattan Bridge, NE corner	584814	4507747	1632.9	174
BW-10-SE	40.73164	-73.9914	Broadway and E 10th St., SE corner	585169	4509456	531.8	80
BW-13-SE	40.73388	-73.9909	Broadway and E 13th St., SE corner	585211	4509705	658.1	59
BW-4-SE	40.72831	-73.9942	Broadway and E 4th ST., SE corner	584936	4509084	409.4	134
BW-8-NW	40.73067	-73.9925	Broadway and 8th Avenue, NW corner	585081	4509347	437.7	93
BW-BK-NE	40.72655	-73.9957	Broadway and Bleeker St., NE corner	584811	4508887	512	160
BW-CN-NE	40.71944	-74.0017	Broadway and Canal St, NE corner	584312	4508092	1321.4	194
C-10-SW	40.72586	-73.9777	Avenue C and E 10th St., SW corner	586333	4508828	1774.1	107
C-14-SW	40.72841	-73.9759	Avenue C and E 14th St., SW corner	586483	4509112	1857.1	98
C-4-SW	40.72228	-73.9803	Avenue C and E 4th St., SW corner	586116	4508427	1748.7	122
C-8-SW	40.72468	-73.9786	Avenue C and E. 8th St., SW corner	586261	4508696	1752.2	112
CH-DL-E	40.71994	-73.9928	Chryste St. and E Delancy St., E median	585069	4508155	1288.1	160
C-HO-W	40.72079	-73.9815	Avenue C and E Houston St., West Median	586019	4508261	1767.1	128
EX-DL-E	40.71852	-73.9881	Essex St. and E Delancey st., E median	585465	4508003	1595.5	149

Location ID	Latitude	Longitude	Description	UTM - Easting	UTM - Northing	Distance to Release Point (meters)	Bearing from Release Point
LF-CN-NE	40.71847	-74.0004	Lafayette St. and Canal St, NE corner	584428	4507985	1402.7	188
LF-HO-E	40.72506	-73.9952	Lafayette St. and E. Houston St., E median	584855	4508722	682.4	161
LF-KM-NE	40.72164	-73.9976	Lafayette St. and Kenmare St., NW corner	584653	4508339	1032	179
LG-3-HE-N	40.72884	-73.9967	Lagardia St and 3rd St, half block E, N side	584720	4509140	243.2	161
LG-BK-NW	40.72818	-73.999	Lagardia St and Bleeker St, NW corner	584530	4509064	327.5	200
LG-HO-W	40.72699	-74	LaGuardia PL and W. Houston St., West median	584448	4508931	481.7	204
PT-DL-W	40.71705	-73.9832	Pitt St. and E Delancey St, E median	585876	4507845	1961.2	141
RLOC-10W-10N	40.73072	-73.9976	Near release point	584645	4509348	23	177
SV-BK-HE-N	40.72865	-74	Sullivan St. and Bleeker St, half block to E, N side	584447	4509116	322.2	217
SV-HO-SE	40.7275	-74.0014	Sullivan St. and Houston, SW corner	584327	4508986	498.7	219
Th-4-SE	40.7302	-73.9981	Thompson St and W 4th St, SE corner	584607	4509290	89.1	204
WB-BR-SE	40.72321	-74.003	West Broadway and Broom St., SE corner	584202	4508509	968.7	207
WB-CN-NE	40.7214	-74.0045	West Broadway and W Canal St., NE corner	584078	4508306	1206.1	207
WBW-BK-HE-N	40.7244	-74.0015	Half block east of West Broadway and Bleeker, N side	584328	4508642	794.5	203
WP-MC-SW	40.729	-73.9939	Washington PL and Mercer St., SW corner	584960	4509161	379.4	123
WSE-WP-HE-S	40.72989	-73.9957	Half block E of Washington Square E and Washington PL, S side	584807	4509258	198.3	124
WS-PR-HE-N	40.72523	-73.9996	Half block east of Wooster St. and Prince St, N side	584480	4508736	655.8	194
WSW-4-NW	40.73111	-73.9996	Washington Square West and W 4th St., NW corner	584475	4509389	170	276
WSW-WSN-NW	40.73231	-73.9986	Washington Square West and Washington Square North, NW corner	584556	4509523	175.6	329

# **Pacific Northwest National Laboratory**

902 Battelle Boulevard  
P.O. Box 999  
Richland, WA 99354

1-888-375-PNNL (7665)

***[www.pnnl.gov](http://www.pnnl.gov)***